Universidade de Aveiro
2016
Departamento de Engenharia de Materiais e Cerâmica

Manuel João Salazar Guedes de Barros

Fabrico de *scaffolds* compósitos de hidrogel e vidro bioativo para regeneração óssea

Universidade de Aveiro
2016
Departamento de Engenharia de Materiais e Cerâmica

Manuel João Salazar Guedes de Barros

Fabrico de *scaffolds* compósitos de hidrogel e vidro bioativo para regeneração óssea

Fabrication of hydrogel-bioactive glass composite scaffolds for bone tissue engineering

Tese apresentada à Universidade de Aveiro para cumprimento dos requisitos necessários à obtenção do grau de Mestre em Materiais e Dispositivos Biomédicos, realizada sob a orientação científica do Doutor Pedro Lopes Granja, Professor Associado do Instituto de Ciências Biomédicas Abel Salazar da Universidade do Porto, do Professor Doutor José Maria da Fonte Ferreira, Professor Associado com Agregação do Departamento de Engenharia de Materiais e Cerâmica da Universidade de Aveiro e do Doutor Hugo Alexandre Gonçalves da Rocha Fernandes, Pós-Doc do Departamento de Engenharia de Materiais e Cerâmica da Universidade de Aveiro.

o júri

presidente

Prof. Doutor Francisco Manuel Lemos Amado
professor associado com agregação da Universidade de Aveiro

Prof. Doutor João Filipe Colardelle da Luz Mano
professor catedrático da Universidade de Aveiro

Prof. Doutor Pedro Lopes Granja
professor associado do Instituto de Ciências Biomédicas Abel Salazar, Universidade do Porto

agradecimentos

Este pequeno espaço não me permite agradecer devidamente a todas as pessoas que fizeram parte da minha vida durante este projeto e que o tornaram possível. Contudo, não queria que a oportunidade de o fazer escapasse apenas por limitações de espaço, pelo que deixo aqui algumas palavras de gratidão e reconhecimento.

Em primeiro lugar gostaria de agradecer aos meus orientadores por todo o apoio prestado durante o decorrer trabalho, pela disponibilidade, críticas, colaboração e oportunidades que me ofereceram, e me ajudaram, mais do que a tornar este trabalho uma realidade, a crescer como investigador e como pessoa.

Agradeço também ao Professor Manuel Azenha da Faculdade de Ciências da Universidade do Porto pela simpatia e disponibilidade para realizar os ensaios espectrofotométricos num tão curto espaço de tempo.

A todo o pessoal do DEMAC o meu obrigado pelo apoio inicial e por sempre me receberem com um sorriso. Gostaria de agradecer especialmente à Catarina, que, mais que uma colega, se tornou uma amiga que me acompanhou quase diariamente em contexto laboral e pessoal, e que contribuiu para este projeto mais do que imagina.

Um obrigado também aos meus colegas de laboratório, tanto do 107 como dos restantes do i3S, pois tornaram a minha chegada mais fácil pela forma como me receberam. Em especial, agradeço à Filipa, que me guiou durante todo o trabalho, que tanta paciência teve comigo e que tanto fez por mim. E como o seu contributo foi maior do que apenas de orientação no laboratório, agradeço-lhe também o bom humor, as piadas, os momentos de troça e descontração dentro e fora do 107.

Aos meus amigos agradeço as palavras de ânimo e o apoio que me prestaram nas horas livres, independentemente do meu cansaço ou mau humor durante este longo percurso. Aos meus colegas de mestrado e aos meus colegas de bancada, obrigado por se tornarem, também, meus amigos.

Por fim, à minha família agradeço a preocupação, os carinhos e as palavras de incentivo que me permitiram alcançar este objetivo. Estou especialmente grato à minha mãe por ser sempre o meu suporte, e pelos constantes exemplos de força, determinação, criatividade, rigor, bondade e tantas outras qualidades que não caberiam nesta página. Assim, a ela lhe dedico este trabalho.

palavras-chave Engenharia de tecidos, hidrogéis, pectina, vidro bioativo.

resumo

O osso é um tecido conjuntivo de extrema importância no organismo humano, tendo funções como suporte ou proteção de órgãos internos, sendo também metabolicamente relevante como o principal reservatório de minerais e assegurando a hematopoiese com a medula óssea. Dado o envelhecimento da população, tem-se verificado um aumento da incidência de doenças degenerativas deste tecido, sendo assim essencial aplicar terapias altamente eficientes para o tratamento dessas patologias. A Engenharia de Tecidos surge como uma tecnologia promissora no tratamento destes problemas, como a perda de massa óssea e problemas nas articulações.

Neste trabalho, foram produzidos biomateriais compósitos, baseados numa matriz polimérica sob a forma de hidrogel reforçada com partículas de vidro bioativo. Individualmente, estes materiais apresentam um elevado teor em água favorável ao transporte de nutrientes, e propriedades osteogénicas, respetivamente. O polímero selecionado foi a pectina funcionalizada com RGD, dadas as suas propriedades interessantes como a biocompatibilidade, capacidade de promover a adesão celular e adequabilidade para o encapsulamento de células, e o vidro bioativo apresenta uma composição de 70% de diópsido e 30% de fosfato tricálcico (Di-70) isento de alcalinos e sendo composto por SiO_2, CaO, MgO e P_2O_5.

Diferentes formulações de hidrogéis compósitos foram testadas, em que se variou a concentração de polímero, a concentração de biovidro e o seu tamanho de partícula. Analisaram-se as propriedades viscoelásticas dos biocompósitos, bem como o seu comportamento biológico, com ensaios de citotoxicidade, e ainda as propriedades osteogénicas do material, pela incubação de hidrogéis contendo células estaminais mesenquimais (MSCs) em meio basal e osteogénico durante 21 dias. Os resultados deste trabalho indicam que foi possível preparar um biomaterial compósito de propriedades mecânicas ajustáveis, com capacidade de reticular *in situ* em tempos clinicamente desejáveis sem necessitar agentes reticulantes externos. Para além disso, as propriedades osteogénicas intrínsecas do biovidro forneceram as condições adequadas para a promoção da diferenciação de MSCs sem estimulação osteogénica adicional. As propriedades combinadas alcançadas indicam que os biocompósitos preparados têm potencial para ser aplicados em engenharia de tecido ósseo.

keywords Tissue Engineering, hydrogels, pectin, bioactive glasses.

abstract

Bone is an extremely important connective tissue in the human body, as it provides support and protection of internal organs, being also metabolically relevant as the main mineral reservoir and assuring haematopoiesis through the bone marrow. Due to the current ageing of the population, an increase in bone tissue related diseases is noticeable. Thus, more efficient therapies for treating bone diseases is crucial. Tissue Engineering appears as a promising technology for treating several of those problems, such as bone loss and joint problems.

In the present work, composite biomaterials composed of a polymeric hydrogel matrix reinforced with bioactive glass particles were prepared. Individually, these materials have a high water content, which enhances their diffusive transport properties, and display osteogenic properties, respectively. The selected polymer was RGD functionalized pectin, due to its interesting properties, such as biocompatibility, cell-adhesive characteristics and adequacy for cell entrapment, and the bioactive glass selected was a novel alkali-free formulation of 70% diopside and 30% tricalcium phosphate (Di-70), composed of SiO_2, CaO, MgO and P_2O_5.

Several different composite formulations were tested, in which pectin concentration, bioactive glass content and glass particle size were varied. The biocomposite's viscoelastic properties were assessed, as well as their biological behaviour through cytotoxicity assays, and osteogenic character by incubating mesenchymal stem cell (MSC)-laden composites into both basal and osteogenic media for up to 21 days. The results obtained demonstrated that a composite biomaterial with tuneable mechanical properties was successfully prepared, with *in situ* crosslinking ability within therapeutically relevant timeframes, and not requiring additional crosslinking strategies besides its own composition. Furthermore, its intrinsic osteogenic properties due to the glass composition provided the adequate conditions for promoting the differentiation of MSCs without osteogenic stimulation. The combined properties achieved indicate that the biocomposites prepared are suitable candidate cellularized biomaterials for bone tissue engineering applications.

Table of Contents

List of Figures

List of Tables

– This page was intentionally left blank –

List of Abbreviations

α-MEM	Minimum Essential Medium α
AM	Additive Manufacturing
BLKpec	Blank Pectin (non-functionalized with RGD)
BSA	Bovine Serum Albumin
CAD	Computer Assisted Design
DAPI	4',6-diamino-2-phenylindole dihydrochloride
Di	Diopside
Di-70	Bioactive glass designation
DM	Degree of methylation
DMEM	Dulbecco's Modified Eagle Medium
F-actin	Filamentous actin
FBS	Fetal Bovine Serum
GalA	(1-4)-linked-α-D-galacturonic acid
GDL	D-glucono-δ-lactone
HA	Hydroxyapatite
hDNFs	Human Dermal Neonatal Fibroblasts
hMSCs	Human Mesenchymal Stem Cell
LVR	Linear Viscoelastic Region
P/S	Penicillin/Streptomycin
PBS	Phosphate-buffered saline
PFA	Paraformaldehyde
PTFE	Polytetrafluoroethylene
RGD	Arginine-Glycine-Aspartic acid amino acid sequence
RGDpec	Pectin functionalized with RGD
SBF	Simulated body fluid
SCPL	*Solvent Casting / Particle Leaching*
TBS	Tris-buffered saline
TCP	Tricalcium phosphate
TE	Tissue Engineering
XRD	X-ray diffraction

– This page was intentionally left blank –

Chapter 1

Introduction

1.1 Framework

In the last century an increase in life expectancy has been observed, especially in developed countries, due to the advances in medicine and medical technology in general [1]. However, this rise in life span also results in population ageing which, aggravated by a sedentary lifestyle, results in an increase in the incidence of degenerative musculoskeletal diseases such as osteoarthritis and osteoporosis. Therefore, there is a growing need for highly efficient treatments for these bone diseases, this constituting the driving force towards the development of new and improved bone regeneration strategies, namely grafts and scaffold materials for application in regenerative medicine [1, 2].

Tissue engineering (TE) is a viable option for the treatment of the aforementioned illnesses, combining the principles of engineering, biology and chemistry in order to obtain a biological substitute that restores, maintains or improves a damaged tissue or organ. This multidisciplinary field combines living cells, biologically active molecules and a physical support in the form of a scaffold to promote cell migration, colonization, growth and differentiation, as well as to increase vascularization and thus allow the ingrowth of new tissues [1-3].

Scaffolds for TE should present a three-dimensional porous structure (with adequate pore size and interconnectivity), suitable mechanical properties matching those of the host tissue in which they will be implanted and they should be biodegradable, ideally with a degradation rate as similar as possible to new tissue regeneration rate [1, 4]. As such, the scaffold's material choice is of extreme importance, as they should fulfil these

requirements, and additionally be biocompatible, i.e., not eliciting any adverse reactions, namely immune reaction in order to avoid acute inflammatory responses that compromise healing or cause rejection by the body, besides allowing for cells to adhere, proliferate and grow without compromising their normal metabolic activity [5].

In bone tissue engineering there are several materials that meet the above requirements and show favourable results, especially polymers and ceramics. Ceramic scaffolds made of calcium phosphates or bioactive glasses, for example, have appropriate mechanical properties for bone applications, as well as excellent chemical compatibility, due to the similarity with bone's structural composition [1, 5]. On the other hand, natural polymeric hydrogels such as collagen, alginate and pectin, have also been widely used in biomedical applications, mainly due to their biodegradability, versatility in terms of biochemical composition and processability, and consequent adequacy as cell carriers [5, 6]. The possibility to create composite materials merging two or more different materials combines each separate material's relevant properties and attenuates their disadvantages. Moreover, bone is intrinsically a composite material, whose structure is mainly composed of hydroxyapatite and collagen, making composite scaffolds attractive options for bone TE [7].

The processing technique is also an important step in developing a material for TE, as it can greatly influence the final properties of the materials. It is essential for the method not to negatively influence the material's inherent properties, such as biocompatibility or chemistry, and it should also provide accurate and consistent processing, avoiding batch to batch variability when scaffolds are processed with the same conditions and parameters [8].

1.2 Objectives

The present work aims at the production of three-dimensional structures made of a natural polymeric hydrogel reinforced with bioactive glass particles and the evaluation of their mechanical and biological properties to assess their suitability for bone tissue engineering applications.

The specific objectives include: i) preparation and processing of the scaffolds' raw materials (pectin and bioactive glass); ii) production composite hydrogels with different formulations in terms of polymer and glass content and glass particle size; iii) characterization of composite's rheological properties and swelling profiles; iv) cell entrapment within the composites and evaluation of their biological behaviour through *in vitro* assays of cytotoxicity, metabolic activity, proliferation and differentiation.

1.3 Dissertation Structure

The present dissertation is divided into 5 main chapters. In **Chapter 1** the framework of the dissertation and its objectives are presented. **Chapter 2** includes a relevant literature review in order to provide context and explain and justify the relevance of this work. **Chapter 3** covers the materials and methods used in the experimental part of the project, including details about the production and processing of materials, and the methodologies used to characterize them, including the biological *in vitro* tests. In **Chapter 4** the results obtained are presented, analysed and discussed. Finally, **Chapter 5** will serve as a conclusion to the work carried out, compiling and summarizing the obtained data, allowing for an introspection of the main aspects learnt and includes proposals of possible future work.

– This page was intentionally left blank –

Chapter 2

Literature Review

2.1 The bone

Bone, alongside cartilage, ligaments, tendons and joints, form the skeletal system, which is responsible for the support and protection of inner organs of the human body, for allowing the movement of the body, for storing minerals and for producing blood cells in the bone marrow. The average adult skeleton has 206 bones distributed along the whole body: skull, torso and limbs. This number may vary person to person, and tends to decrease with age due to fusion of some bones [9].

Just as other connective tissues, bone tissue consists of cells and extracellular matrix. This matrix is composed of approximately 35% organic material (mainly collagen and proteoglycans) and 65% inorganic material (primarily a calcium phosphate called hydroxyapatite (HA), with the molecular formula $Ca_{10}(PO_4)_6(OH)_2$). Bone properties are highly influenced by the equilibrium of these constituents, as collagen provides flexibility and the mineral component offers compression strength. On one hand, if the organic part is removed, bone becomes very brittle and, on the other hand, if the minerals are removed, it will become overly flexible [9].

Bone cells control bone functions and can be categorized into three different types: osteoblasts, osteoclasts and osteocytes. Osteoblasts are responsible for the production of new bone matrix in a process called osteogenesis (or ossification). These cells remain active for about eight days, producing fibres and matrix until they are completely surrounded by extracellular matrix, maturing and developing into osteocytes, which are sensitive to mechanical stimuli and maintain the bone matrix. Osteoclasts are responsible

for the resorption of bone. An equilibrium between osteoblastic and osteoclastic activity is essential to preserve bone properties, in a process called bone remodelling [9, 10].

It is also essential to distinguish between compact (or cortical) and spongy (or cancellous) bone (**Figure 1**), which are the two macroscopic types of bone tissue. Spongy bone has a porous appearance and consists of a fine net of interconnecting bone rods called trabeculae. In long bones, the spaces between trabeculae hold blood vessels that irrigate the bone and bone marrow, allowing for a higher remodelling rate than that of the compact bone. This latter class of bone is much denser and has fewer spaces than spongy bone. It is constituted by concentric lamellae that surround blood vessels, forming structures named osteons. About 80% of total bone mass is constituted by compact bone [9, 10]. As a consequence, these two types of bone display very different characteristics, including very distinctive mechanical properties, contributing to the tissue's torsional, flexible and compressive strengths [10]. **Table 1** summarizes some of those properties.

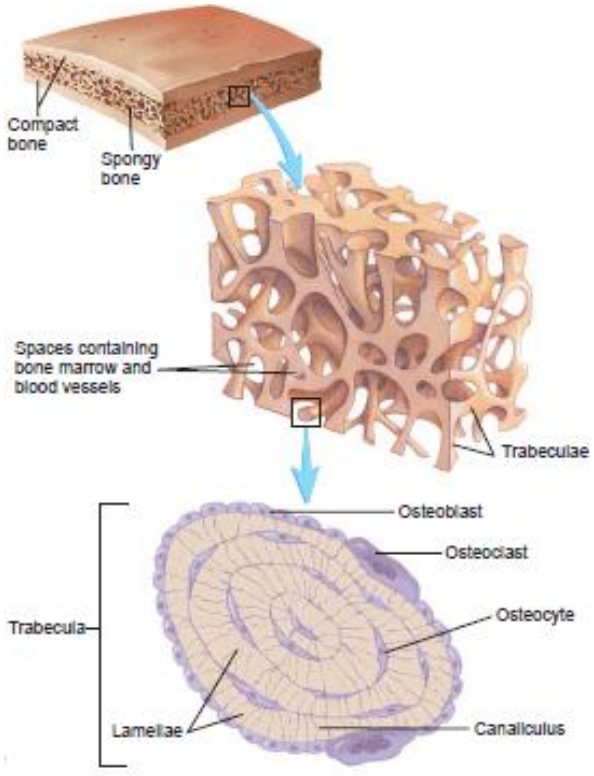

Figure 1 *– Spongy bone structure (Adapted from [9])*

Table 1 – Mechanical properties of compact and spongy bone (Adapted from [11]).

Mechanical property	Compact bone	Spongy bone
Compressive strength (MPa)	130 – 200	0.1 – 16
Compressive modulus (GPa)	11.5 – 17	0.12 – 1.1
Young's modulus (GPa)	7 – 30	0.05 – 0.5

Bone's mechanical properties are influenced by several factors such as age, gender and general health of the individual. This fact, associated with the fact that bone is an anisotropic material, which results in variable mechanical properties according to the load's direction, might explain the inconsistency of mechanical properties' values found in the literature [10].

Bones can also be classified according to their shape. They can be long (such as the femur and the ulna), short (including carpal and tarsal bones, with nearly cubic shapes), flat (like the ones found in the skull) or irregular (such as the vertebrae). Long bones are composed by different parts, namely the diaphysis, the epiphysis and, in growing bones, the epiphyseal plates. These cartilaginous plates are replaced by bone in structures called epiphyseal lines when bone growth stops (**Figure 2**). The diaphysis can be considered the body of the bone and is primarily composed of compact bone; on the other hand, the epiphysis is composed of spongy bone with an external layer of compact bone. In long bones' diaphysis there can be a large internal space called the medullary cavity, which is filled with yellow bone marrow [9]. Due to being more susceptible to bending moments, long bones are more prone to suffer fractures [10].

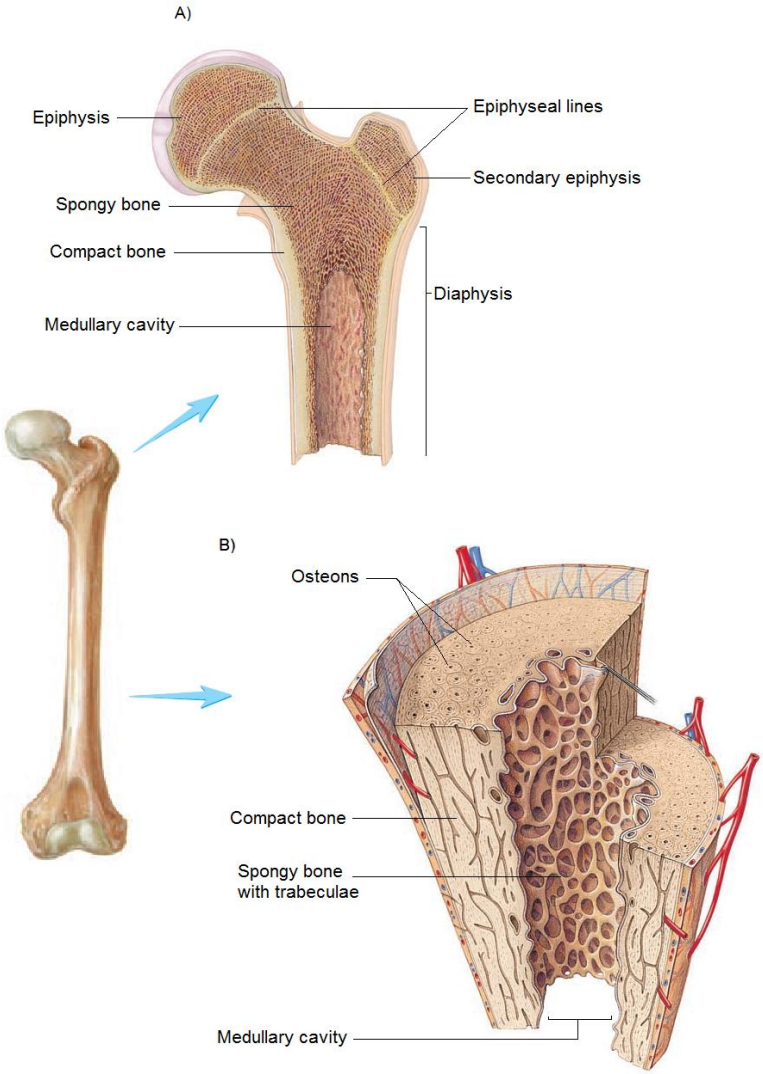

Figure 2 *– Structure of an adult long bone (femur): A) Epiphysis; B) Internal features of the diaphysis (Adapted from [9])*

Due to the combination of the above described characteristics, bones are one of the hardest and sturdiest structures in the human body, second only to dentin's enamel. They are also one of the most dynamic and metabolically active tissues, displaying activity throughout all stages of life. Bones are sensitive to mechanical loads, which can alter their density, configuration and general properties, and exhibit an excellent self-reparation capability in case of trauma or fracture [10].

2.1.1 Bone renewal and remodelling

Bones can remodel, i.e., they can adjust by resorbing old tissue and producing new bone tissue in different places, modifying their morphology according to the varying mechanical conditions they are exposed to. Osteocytes, as mentioned before, have a predominant role in this process due to being sensitive to mechanical stimuli [10]. Bone remodelling is linked to bone growth and is influenced by genetic factors, nutrition and hormones [9]. Bone growth's processes (resorption and formation of bone tissue) are not balanced, resulting in shape, mass and microarchitecture modifications [10].

Annually, around 10% of total bone mass is replaced in adults due to the remodelling process, which helps prevent the accumulation of microfissures, thus repairing the small damage induced by the cyclic mechanical stress applied to the bones. Moreover, bone remodelling helps to maintain optimal calcium levels in the blood [10]. This process, as mentioned earlier, is reliant on a coordination of osteoblastic and osteoclastic activity. These cells form temporary assemblies called basic multicellular units that travel through and across the surface of the bone, removing old matrix and replacing it with new one, which lets the tissue renew itself without changing its morphology or density [10, 12]. It is a mechanism that includes a sequence of well-defined events that include the activation of osteoclasts with consequential resorption of bone tissue, followed by osteoblasts' activation which will form new bone at the site of resorption [12]. Remodelling rates vary throughout life, being higher during childhood. It is also greater (about five times) in spongy bone compared to compact bone [10].

These processes are of extreme importance in order to maintain bone properties and repair small defects. However, for larger defects, human intervention is required to aid or stimulate the healing [12].

2.1.2 Bone defect repair

The natural process of bone fracture recovery is a complex procedure that begins as soon as the fracture occurs, evolving towards its consolidation. This mechanism is different for compact bone and for spongy bone. For the former, the process is similar to the scar

formation in the healing process of a skin wound. Bone's vascularization plays a crucial role, as different vessels may be affected depending on fracture site [10].

The repairing process of a long bone has three main stages: the inflammatory phase, the repair phase and the remodelling phase (**Figure 3**). The first stage has a two to three-week duration and leads to the formation of a hematoma, as a result of surrounding blood vessel damage, followed by an inflammatory reaction. Fractured surfaces can also suffer necrosis, which extent depends on the degree of soft tissue damage and on the distance separating the affected surfaces. After the hematoma, a clot is formed to stop the bleeding. Afterwards, the recovery phase begins with the formation of the callus, which connects the broken ends of the bone, promoting their union. The callus forms as the clot dissolves, between the fourth and eighth week after the fracture happens. It has an internal component, which replaces the hematoma, and an external component that helps stabilize the bone. At this point, immobilization of the fracture site is crucial to avoid complications due to excessive movement. Then, ossification of the callus occurs by the deposition of new collagenous matrix and calcium phosphate salts, which creates an immature, woven bone with no well-defined structure. Finally, the bone remodelling process initiates, allowing the woven and necrotic bones to be replaced with new compact bone, completing the fracture repair process [9, 10].

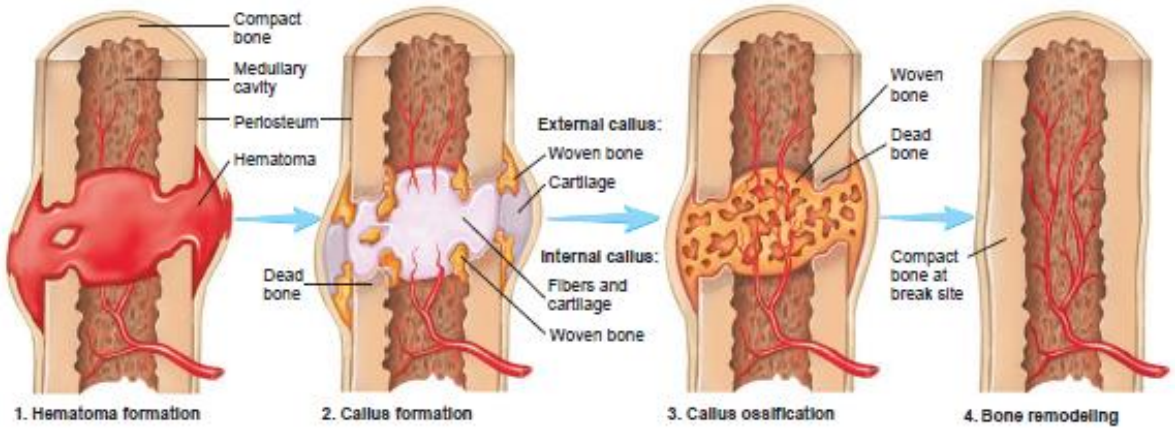

Figure 3 *– Stages of bone fracture repair process (Adapted from [9])*

Hence, bone defect repair is a biologically and mechanically complex process which can and should be facilitated by human intervention. There are several different

approaches to help repair an injured bone, such as bone grafts (natural or artificial) or tissue engineering (TE) strategies. Natural grafts can be divided into three major categories: autografts, allografts and xenografts. Each option offers different advantages and disadvantages [13]. Autografts remain the gold standard in many small defect cases, and coming from another part of the patient's body, they minimize incompatibility issues or disease transmission risk. They present ideal osteogenic properties, but require two different surgeries, which encompass two separate scarring processes, increases infection risk and result in high pain and donor site morbidity, as well as higher blood loss [13-16]. Allografts are a common alternative to autografts due to reducing the morbidity of the process, since they are obtained from a different individual of the same species. Another benefit of the use of allografts is the possibility to perform local anaesthesia. However, these grafts have inferior osteogenic and osteoinductive properties, and their processing also weakens their biological and mechanical properties. Furthermore, they are more likely to induce immune system response and face other problems regarding ethics and waiting lists [13, 17, 18]. Finally, the last natural option are xenografts, whose source is an individual from another species. The main advantages of the use of xenografts include the low costs and the highly available resources associated. However, they carry the same disadvantages as allografts, and additionally carry the risk of zoonotic diseases transmission and are more likely to be aggressively rejected by the body [13, 19, 20].

Artificial grafts, or synthetic biomaterial-based substitutes, have been showing promise in decreasing natural graft's drawbacks [13]. An artificial bone graft can be defined as an implantable material that promotes the regeneration of bone tissue via osteogenesis, osteoinduction and osteoconduction. These grafts can have different origins, and the selection depends on several factors including tissue viability, defect size (as well as its shape and volume), biological and biomechanical properties, cost and ethical issues [13]. The most commonly used artificial grafts in bone TE are either polymeric (such as collagen, chitosan, alginate or polylactic acid) or ceramic (for instance, bioactive glasses, HA or different calcium phosphates) and even though they show promising results, the low mechanical properties, reduced osteogenic properties and unpredictable dissolution rates hinder their usability [13, 21].

To circumvent the above-mentioned drawbacks of natural and artificial grafts, TE strategies and the development of novel materials and technologies provide new and improved alternatives for efficient bone regeneration.

2.2 Tissue engineering

Tissue engineering is an expanding field whose objective is the production of biological substitutes that restore or improve tissue and organ function. The term "Tissue engineering" was defined by Langer and Vacanti as a multidisciplinary field that applies engineering and life science's principles and methods to better understand the connection between tissue structure and function and to develop biological substitutes that repair, maintain or improve tissues [5, 22]. Hence, this branch of regenerative medicine presents itself as an interdisciplinary field that combines knowledge from medicine, engineering, materials science, chemistry, genetics, biology and all related [5, 23].

The basis of TE is the combination of live cells, biologically active molecules (for example, growth factors, hormones or genes) and a three-dimensional construct capable of supporting the colonization, migration, growth and differentiation of cells in order to regenerate malfunctioning tissues (**Figure 4**) [1].

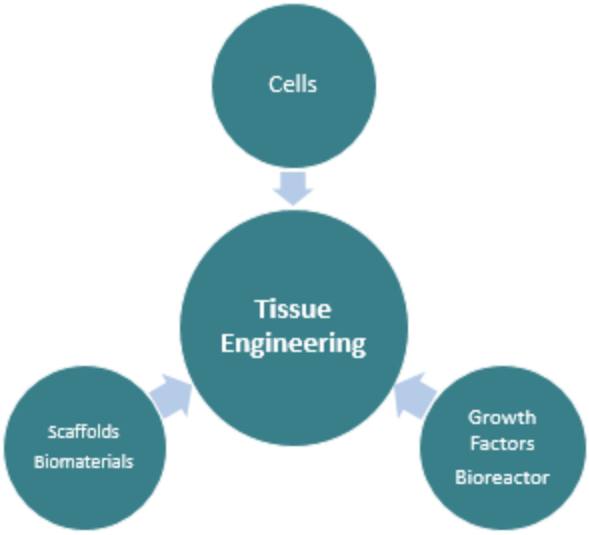

Figure 4 – *Principles of Tissue Engineering (Adapted from [5]).*

The three-dimensional structure is obtained through the construction of a scaffold that works as a physical support for cells, providing an application-specific microenvironment, as well as serving as water, nutrients and other important molecules reservoir [8]. These constructs must be biocompatible, biodegradable and should have appropriate mechanical properties and architecture. It is also required that processing techniques do not negatively influence the scaffolds' characteristics [5].

Biocompatibility is a vital criterion that must be fulfilled by any biomaterial for TE. It is described as the ability of a material to induce cell adherence to its surface, allowing them to proliferate and differentiate, without causing an acute inflammatory reaction at the time of implantation that could possibly compromise the success of the therapy through reduction of healing capability or material rejection [5, 22].

Biodegradability is also a fundamental characteristic of scaffolds used in TE, as its main goal is to aid patient's self-healing process. As such, and ideally, the degradation rate of implanted scaffolds should be as close as possible to host tissue's regenerative rate, namely extracellular matrix production by the cells. It is essential that the by-products of their degradation are non-toxic as well, and they should be able to easily exit the body without interfering with other organs [5, 24, 25].

Scaffolds' mechanical properties should mimic, as far as possible, the properties of the tissue they will be implanted on, this remaining one of the biggest challenges in TE, especially in cardiovascular and orthopaedic applications. They should also be resistant to the handling during the surgical implantation [3, 5]. In bone tissue regeneration, one consequence of the discrepancy between the mechanical properties of the bone and the biomaterial is designated as stress-shielding effect, which can be described as an adaptation of the host tissue to constant localized disuse as a result of reduced mechanical stimuli. This causes a higher resorption of bone tissue at the area surrounding the implant, leading to bone mass loss [10].

The design of the scaffold is also extremely important. Scaffolds should be highly porous so as to increase its surface area and to enable cell proliferation, tissue vascularisation and adequate oxygenation. The pores should also be interconnected in order to allow for cell migration and proper angiogenesis [5]. Pore size may vary, being that both micro and macroporosity influence osteogenesis [8].

Scaffold fabrication technique is another relevant factor to take into consideration, since it should be possible to scale-up from making single units into producing bigger batches without affecting the economic viability of the process, in order to create a clinically and commercially sustainable material [5].

The three-dimensional structure is especially important since tissues and organs are three-dimensional as well. This more complex morphology is crucial in maintaining cell viability, influencing their shape, gene expression, growth, mobility and differentiation, as cells and their extracellular matrix interact strongly. All these features can also be regulated with the addition of growth factors, cell adhesion molecules or hormones to the material's composition [26, 27].

Growth factors and hormones are biomolecules capable of stimulating new bone formation, for example, by enhancing osteogenesis and angiogenesis [28, 29]. Bhattacharjee *et al.* (2016) showed that the use of a combination of different growth factors (transforming growth factor beta and bone morphogenetic protein-2) lead to an increase in MG-63 cell activity, proliferation and differentiation, higher calcium deposition and greater expression of bone growth related genes [30].

Some scaffold materials do not intrinsically interact with cells. In that case, it is possible to potentiate cell adhesion by modifying the material with molecules such as peptides containing the amino acid sequence arginine-glycine-aspartic acid (RGD), which interacts with the integrins present in cell's cytoplasmic membrane [24, 31].

The choice of the cells to use in TE applications also influences the therapeutic success. Stem cells, and specifically human mesenchymal stem cells (hMSCs), have been recognized as a promising cell source for bone tissue engineering. When under appropriate *in vitro* conditions (within ceramic or polymeric matrixes with the adequate characteristics), these multipotent progenitor cells can be induced to differentiate into adipocytes, chondrocytes or osteoblasts [32, 33].

Thus, TE allows for a great amount of possibilities, depending on the desired application. As such, the choice of biomaterials to use should be taken into account, as they are a central part of these therapies.

2.3 Biomaterials

According to the American National Institutes of Health, a biomaterial is any natural or synthetic substance or combination of substances, other than drugs, that can be used for any amount of time, and whose purpose is to totally or partially enhance or replace any tissue, organ or function in order to improve the quality of life of an individual [34].

Biomaterials can be classified into the four main classes of materials, i.e., metals, ceramics, polymers and composites, differing in their properties and possible applications. Metals are strong and usually inert materials but who suffer from oxidation [34]. Ceramics can be of natural (for instance, HA) or synthetic (such as bioactive glasses) origin, and are very hard but brittle materials who often show bioactivity and biodegradability [34-36]. Polymeric materials, as ceramics, can be natural (collagen and chitosan for example) or synthetic (polylactic acid, polycaprolactone, polymethyl methacrylate among others). They are light, versatile and often biodegradable materials [34, 35]. Finally, composites are materials that combine two or more different materials, assembling the positive characteristics of each component and overcoming their limitations [34, 35, 37-39].

Biomaterial usage began around 1950, where the materials were mainly inert and selected for provoking minimal reactions in the host tissue. This is considered the first generation of biomaterials, and an example of a successful application is the total hip replacement still currently practiced. One of the materials used for total hip replacements at the time was austenitic stainless steel, as it was resistant to corrosion and showed appealing mechanical properties [34].

The second generation of biomaterials began around 1970 with the need to find materials that would interact with living tissues. Novel bioactive materials emerged in this generation of biomaterials, used either as bulk or as coatings for other materials, in order to improve the implant-tissue interface [34, 40].

Alongside the concept of tissue engineering, the third generation of biomaterials arose, in which the material's main goal was to enhance tissues' self-regeneration instead of simply replacing them [34, 41].

All biomaterials share common features, such as being biocompatible, biofunctional, i.e., having adequate physical and chemical properties for their desired

application, as well as being sterilizable [34]. Sterilization is indispensable for any surgically inserted material in the human body, and can be a problematic process for some materials, namely polymeric ones, as some traditional sterilization techniques may alter some of their properties in undesirable ways [42].

Some materials may also be bioactive, as mentioned previously. This feature is mostly found in ceramics and can be defined as a material's ability to interact and bond to surrounding tissues, generating an environment that is favourable to osteogenesis. Bioactive implants and grafts form a layer of hydroxyapatite at the surface, creating a strong interface between bone and material [43].

Thereby, biomaterials can be classified according to the type of interaction with the host tissue, as summarized in **Table 2**.

Table 2 – Types of implant-tissue interactions (Adapted from [43])

Property	Type of attachment	Biomaterial
Nearly inert	Morphological fixation (mechanical interlock)	Metals, alumina, zirconia, polyethylene
Porous	Biological fixation (growth of tissues into the pores)	Hydroxyapatite, coated porous materials
Bioactive	Bioactive fixation (interfacial bonding with tissues)	Bioactive glasses, hydroxyapatite, glass-ceramics
Resorbable	Replacement of the material with new tissue	Tricalcium phosphates, polylactic acid

Several biomaterials meet the biological and technological criteria to be used in bone tissue engineering, although ceramic materials are usually favoured. As previously stated, these can be of natural origin (e.g., coralline HA) or synthetic (as β-tricalcium phosphate), and their advantages include osteoconductive and osteoinductive properties [8]. However, their mechanical instability and unpredictable dissolution rates can be problematic, as these factors can contribute to cellular death due to a rise in extracellular calcium and phosphorus concentrations [8, 44].

Bioactive glasses have been gradually introduced as alternatives for bone tissue regeneration because of their development and success since the discovery of 45S5 Bioglass® by Larry Hench [45]. New formulations have been created aiming to improve this material's properties and expand its uses [46]. Section **2.3.1** will develop this topic in more detail. Polymers are also widely used in bone TE, both natural (as collagen, alginate, chitosan and pectin) and synthetic (e.g., PGA, PCL and PLA) [6, 23]. However, and taking into account bone's own composite structure, there has been a growing interest in the use of composite materials for bone tissue engineering. Some formulations consist of calcium phosphate hybrids, such as HA combined with different polymers, showing evidence of promising results in terms of mechanical properties, and with augmented osteogenic ability due to the ceramic's mineralization capabilities [3, 7].

2.3.1 Bioactive glasses

Bioactive glasses were discovered around 1969, when Larry Hench developed the 45S5 Bioglass® [45]. This glass has a specific composition of 45% SiO_2, 24.5% CaO, 24.5% Na_2O and 6% P_2O_5 (wt %), which allows it to establish strong bonds with hard tissues, thus creating the concept of bioactivity. 45S5 Bioglass® is therefore considered by many as the pioneer of bioactive materials, leading to the development of several new formulations [43, 45, 46].

Hench also proposed a series of steps that sequentially describe what happens at the surface of bioactive materials when in physiological environments. They are as follows [47, 48]:

1. Ionic exchange between the material's Na^+ and the fluid's H^+ and H_3O^+;
2. Dissolution of silica into the fluid ($Si(OH)_4$) and establishment of Si–OH bonds at the material's surface;
3. Condensation of the silica-rich coating in the material's surface;
4. Adsorption of Ca + PO_4 + CO_3 + OH to the previously formed silica layer, with development of an amorphous layer rich in CaO and P_2O_5;
5. Crystallization of a carbonated HA layer;
6. Adsorption of biological molecules to the HA surface;

7. Macrophage action;
8. Cell adhesion;
9. Cell differentiation;
10. Extracellular matrix production;
11. Mineralization of the newly formed matrix.

Nevertheless, 45S5 Bioglass® is not free from flaws, as some hindrances have been reported, such as its easy dissolution in an aqueous environment, which leads to a decrease in bioactivity and an increase in pH due to the high sodium concentrations. This fact can hinder natural processes such as bone remodelling, compromising the effectiveness of the therapy [1, 12].

Hence, new formulations of glasses and other bioactive ceramics have been developed and commercialized, in an attempt to overcome its drawbacks [47]. A summarized list of examples of these materials and their compositions is provided in **Table 3**.

Table 3 – Examples of commercialized bioactive glasses and glass-ceramics and their respective compositions (wt %) (Adapted from [46, 47])

Bioactive glasses	SiO_2	P_2O_5	CaO	$Ca(PO_3)_2$	CaF_2	MgO	Na_2O	K_2O	Al_2O_3	B_2O_3	TiO_2
45S5 Bioglass®	45.00	6.00	24.50	-	-	-	24.50	-	-	-	-
45S5.4F Bioglass®	45.00	6.00	14.70	-	9.80	-	24.50	-	-	-	-
45B15S5 Bioglass®	30.00	6.00	24.50	-	-	-	24.50	-	-	15.00	-
52S4.6 Bioglass®	52.00	6.00	21.00	-	-	-	21.00	-	-	-	-
55S4.3 Bioglass®	55.00	6.00	19.50	-	-	-	19.50	-	-	-	-
KGC Ceravital®	46.20	-	20.20	25.50	-	2.90	4.80	0.40	-	-	-
KGS Ceravital®	46.00	-	33.00	16.00	-	-	5.00	-	-	-	-
KGy213 Ceravital®	38.00	-	31.00	13.50	-	-	4.00	-	7.00	-	6.50
A/W glass-ceramic	34.20	16.30	44.90	-	0.50	4.60	-	-	-	-	-
FastOS®BG	38.84	13.37	33.98	-	0.77	13.03	-	-	-	-	-

In the present work, a bioactive glass from the $CaO–MgO–SiO_2–P_2O_5$ system was used. It is based in two components of interest: diopside (Di, $CaO{\cdot}MgO{\cdot}2SiO_2$) and tricalcium phosphate (TCP, $3CaO{\cdot}P_2O_5$). This formulation results in an alkali-free bioactive glass, which offers a slower and more controlled dissolution rate [49]. Diopside is a member of the pyroxenes' class and presents favourable mechanical properties and bioactivity. Additionally, TCP is a resorbable calcium phosphate with known applications in bone tissue engineering for its excellent osteogenic properties [50]. The selected glass composition for this work (70% Di – 30% TCP, wt %) hereafter referred to as Di-70, corresponds to the following molar composition: 36.52% CaO, 19.24% MgO, 38.48% SiO_2 and 5.76% P_2O_5 [49]. Previous studies using this bioactive glass indicate that it is highly bioactive and osteogenic, stimulating the differentiation of mesenchymal stem cells into bone tissue cells [50].

2.3.2 Pectin

In the present work, composite materials prepared from Di-70 bioactive glass and pectin will be produced. Pectin is a naturally derived polymer that constitutes 30% of higher plants' cell walls. It is widely used in the food industry, namely as a stabilizer, emulsifier, thickener and gelling agent [6, 51]. However, it also shows promise in the biomedical and pharmaceutical fields, for instance in colon drug delivery systems, as it is specifically degraded by the anaerobic bacteria present in the intestine. It also shows interesting mucoadhesive properties, forming bonds with the mucin, which allows for a better control of its residence time in the body and enables the use of lower drug concentrations or doses [52, 53]. Its perspective applications include TE and its advantages include the ease of obtention, low cost, biocompatibility, non-toxicity and the fact that it induces the nucleation of mineral phases while under osteogenic conditions [53, 54].

Commercially available pectin is mainly obtained from apple pomace and citrus fruits' peel through an acidic aqueous extraction process [54]. Pectin extracts obtained from plants' cell walls share some common features, being predominantly composed of a homopolymer of (1-4)-linked-α-D-galacturonic acid (GalA) units that can be partially esterified on the carboxyl group and by the acetyl group on the secondary hydroxyls.

Pectins can be classified regarding their degree of methylation (DM), where low-methoxyl pectins present a DM < 50% and high methoxyl pectins show a DM > 50% [51]. This polymer's properties are affected by its molecular weight and degree of esterification, thus the selection of the pectin source should be carefully made, since pectins of different origins may be more or less suitable for biomedical applications [53, 55].

Low-methoxyl pectins in solution can form hydrogels when in the presence of divalent metal ions such as calcium (Ca^{2+}) (**Figure 5**) [51-57]. Calcium ions induce chain-chain associations that constitute junction zones responsible for the formation of gels in a model known as the egg-box model [58].

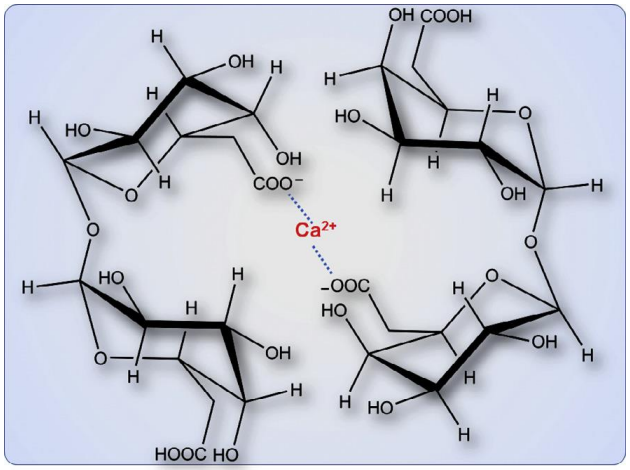

Figure 5 *– Formation of a pectin hydrogel through ionic crosslinking (Adapted from [58])*

Hydrogels are highly hydrated structures composed of hydrophilic polymeric chains that have a wide range of uses in TE due to their similarity to extracellular matrices by virtue of their high water content, which enhances viscoelastic properties and diffusive transport capability [51]. There are two possible methods to produce pectin hydrogels: external and internal gelation. The former is achieved by extruding droplets of a pectin solution into a calcium-rich solution, which allows the production of polymeric particles and beads due to the fast crosslinking reaction [6]. On the other hand, internal gelation allows the fabrication of scaffolds suitable for TE, since it produces homogeneous gels from the mixture of a poorly soluble calcium salt (e.g., calcium carbonate, $CaCO_3$) into the polymeric solution with an acidification mechanism that promotes a slow release of calcium and the resulting crosslinking [6, 51].

RGD-modified alginate and pectin biomaterials, who share many common features (although alginate is more commonly used), have also shown promising results in the differentiation of mesenchymal stem cells into bone cells when cultured in osteogenic conditions by providing an appropriate microenvironment for cellular attachment, growth and proliferation, making them suitable for bone tissue engineering applications by combining them with the bioactive glass [51, 59-63].

2.3.3 Hydrogel and bioactive glass composites

The use of composite materials in bone tissue engineering is a widely studied strategy that shows promising results due to bone's own composite composition. The most common approach is the use of polymer matrices reinforced with calcium phosphates (such as HA and TCP), as the study of bioactive glasses is still a growing field [64-66]. There are several studies focusing on biocomposites of this kind, with varying percentages of ceramic (from 0.1 to up to 87, wt %), different porosities and pore sizes and, consequently, diverse mechanical properties [67-69].

As previously mentioned, both bioactive glasses and hydrogels show interesting and appealing properties for TE. However, these materials present some drawbacks when used alone, which suggests that composites might mitigate those issues. With hybrids of polymers and bioactive glasses, it is possible to obtain materials with more adequate properties for bone tissue engineering, namely in terms of toughness and plasticity (provided by the polymeric phase) and in terms of osteogenic properties and compressive strength (provided by the mineral component) [70]. Moreover, the combination of these two materials is expected to result in an additional benefit, which relies in the crosslinking potential provided by the bioceramic, through the release of calcium and magnesium from its composition, both divalent cations that can induce the formation of the egg-box junctions in the pectin hydrogel [64].

Significant research efforts have been dedicated to develop this type of composites in injectable forms, in which the processing techniques and desired properties are highly different from those designed for three-dimensional scaffolds, especially regarding the rheological profiles, since the final products are microspheres or pastes [60, 70, 71].

Polymer-glass ceramic composite scaffolds for TE may be ceramic-based impregnated with polymers, or polymer-based (for instance, hydrogels) with bioactive glass particles as reinforcement [65]. For the latter, the structure's mesh size, mechanical and thermal properties, polymer-to-ceramic ratios, dissolution profile, ability to promote cell adhesion, mineralization inducing properties, as well as the particles' morphology, size and microstructure are extremely important and need to be taken into consideration when designing a biomaterial [3, 65, 70-72]. More specifically, two major factors that are usually investigated to characterize the biocomposites are the percentage of bioactive glass content and the size of its particles. In general, glass content seems to highly influence the mechanical properties of the materials, which makes it an important parameter to control in order to achieve the desired characteristics, and particle size mainly affects the material's osteogenic ability, in which smaller particles (nanoscale) appear to induce better responses [73-76].

In summary, several diverse formulations have been studied, and some examples include the use of 45S5 Bioglass® with different polymers (such as collagen or gelatine), FastOs®BG with polycaprolactone or even different bioactive glasses with a polymer of bacterial origins (gellan gum), all showing promising results for bone TE [1, 3, 65, 70, 77]. Some studies also report the use of this type of composite for drug delivery therapeutics or the use bioactive glasses doped with metal ions such as copper or strontium with promising results, suggesting that it might be possible to incorporate other compounds with anti-inflammatory, anti-bacterial and angiogenic properties into these composite materials [3, 66, 78]. From the analysis of the literature it is noticeable that pectin and bioactive glass composite scaffolds are still unexplored formulations.

2.4 Processing techniques

After selecting the suitable materials for a specific TE application, it is important to choose the ideal processing technique, taking into account factors such as costs, reproducibility and ability to preserve the raw material's desired properties (such as biocompatibility) [8]. Scaffold production techniques can significantly affect their

characteristics, namely their porosity, degradation rate, as well as mechanical or chemical properties. Furthermore, there are procedures that prevent the use of cells and biologically active compounds due to the high temperatures or pressure values needed for their production [23].

Thus, the choice of the appropriate technique depends on the application and on the desired properties, taking into account that all of them have advantages and disadvantages. The most relevant scaffold fabrication technologies include [23]:

1. Solvent casting/particulate leaching (SCPL), which is based on the dissolution of a material in an organic solvent, followed by the porogen addition, drying process and solidification, followed by porogen removal;
2. Gas-foaming, in which CO_2 is the porogen;
3. Phase separation, which divides a homogeneous solution into two or more separate phases using a thermal treatment;
4. Freeze-drying, where an emulsion is quickly cooled and then the water and other solvents are removed;
5. Electrospinning, whose key-point is the application of high voltage to a polymeric solution and pumping it into a spinneret;
6. Rapid prototyping, which combines computer and materials science in order to form a paste that later sets into a pre-defined shape;
7. Self-assembly, in which the components are autonomously organized without human intervention;
8. Stereo-lithography, that uses UV laser power to harden a photopolymerizable material into a desired shape or pattern;
9. Moulding techniques, in which a mould is filled with the material to give it a set shape.

Some of the main advantages and downsides of each of these techniques are described in **Table 4**.

Table 4 – Advantages and disadvantages of some of the most common scaffold processing techniques (Adapted from [23])

Technique	Advantages	Disadvantages
Solvent casting/particulate leaching	Simple, inexpensive and allows control over porosity and pore size	The use of toxic solvents and limitations in scaffold thickness
Gas-foaming	High porosity and organic solvent-free process	Limited mechanical properties and low pore interconnectivity
Phase separation	Solvent-free technique, controlled porosity and can be used to produce nanofibers	Difficult control of the scaffold micro- and macro-structure and limited material selection
Freeze-drying	Simple, solvent-free, high porosity and pore size control	Slow process and low pore sizes
Electrospinning	Ability to produce fine fibres with special orientations and high surface area in a quick and simple way	Mechanical properties limitations and difficulty in producing scaffolds with complex structures
Rapid prototyping	Highly accurate and reproducible method requiring minimal intervention and allows production of complex structures with controlled properties	Expensive, often requiring high temperatures and organic solvents and limited material selection
Self-assembly	Toxic solvent-free process and allows producing nanofibers	Expensive and limitations in terms of mechanical properties
Stereo-lithography	Allows the production of structures with complex internal features	Limited selection of photopolymerizable materials
Moulding techniques	Solvent-free process providing independent control of porosity and pore size	Difficulties in producing three-dimensional scaffolds, with risk of residual porogen, and high temperatures required

Additive manufacturing (AM) techniques are processing technologies that have altered the way materials are designed, produced and distributed to end users, gaining significant interest in both academic and industrial environments. It is possible to find AM

techniques in different sectors, such as in the automotive and aerospace industries, in electronics, construction, medicine or even in the food industry. One feature that makes these techniques appealing is the ease to produce complex constructions with close to no residual materials, reducing waste [79].

Their ability to produce custom scaffolds makes these techniques interesting for biomedical applications, allowing the production of highly complex materials in a reproducible way. Some of these techniques include 3D printing, stereo-lithography and robocasting, and they are based on the assembly of three-dimensional structures layer-by-layer with the aid of a computer assisted design (CAD) model. An additional advantage of the use of these techniques is the possibility to use medical imaging data, such as X-ray or magnetic resonance imaging scans, to generate a CAD model that translates into a biomaterial that perfectly replicates the defect to repair [80].

There are some examples of scaffolds for bone TE produced using this type of processing technique with promising results, recurring to materials such as HA, polylactic acid, polycaprolactone and some bioactive glasses [81]. However, production of pectin based biocomposites for tissue engineering via AM techniques is a field with much room for development, yet it would of great interest as a future final objective of this project.

– This page was intentionally left blank –

Chapter 3

Materials and Methods

3.1 Materials

The bioactive glass Di-70, whose molar composition is 38.48% SiO_2, 36.52% CaO, 19.24% MgO and 5.76% P_2O_5, was produced using high purity powders, as described in **Table 5**.

Table 5 *–Raw materials used to prepare bioactive glass.*

Material	Brand	Purity
SiO_2	Sibelco	≥99%
$CaCO_3$	Sigma-Aldrich	≥99%
MgO	Sigma-Aldrich	≥98%
NH_6PO_4	Fluka	≥99%

Low-methoxyl citrus pectin (Classic CU701) with a galacturonic acid unit content of 86% and a degree of methylation of 37% was provided by Herbstreith & Fox.

3.2 Glass synthesis and characterization

Homogeneous mixtures of approximately 70 g batches of glass's raw materials were obtained by ball milling for about 10 minutes. Afterwards, the mixture was transferred to alumina crucibles for calcination at 900ºC for 1 hour (2ºC/min rate), after which the material was melted in platinum crucibles for 1 hour at 1570ºC (10ºC/min rate). The glasses were obtained in frit form by quenching the melted glass in cold water. The glass frits were dried in a drying oven at 100ºC for 24 hours prior to being milled in planetary agate ball mill for 2 hours at a speed of 200 rpm (Retsch PM 400).

After that, the resulting fine glass particles were sieved (<500 μm) and their mean size (φ) was determined by a light scattering technique (Coulter LS230, Beckman Coulter; Fraunhofer optical model), being of about 8 μm. Part of the obtained glass particles was stored in a desiccator and the other part was submitted to a wet ball milling process to further decrease mean particle size. The glass powders were milled in ethanol for about 18 hours at a speed of 750 rpm in an attrition mill. These powders with mean particle size of 1 μm were then dried for 24 hours at 100ºC, sieved again (<40 μm) to eliminate agglomerates and stored in a desiccator until further use.

The amorphous/crystalline nature of the glass frits was analysed by X-ray diffraction (XRD) analysis (Rigaku Geigerflex D/Max, Tokyo, Kapan; C Series, CuKα radiation; 2α angle range: 10º–80º; step of 0.02º/s).

3.3 Pectin purification and biofunctionalization

Prior to any studies or modifications, pectin was purified to reduce common contaminants such as proteins, polyphenols and endotoxins [51]. Succinctly, a 1% (w/v) pectin solution was prepared by dissolution of the polymer in HyClone™ endotoxin-free cell culture grade water (GE Healthcare) and its pH was adjusted to 6 using NaOH (1M and 5M, Merck) solutions. Then, the solution was sequentially filtered with 0.80 μm, 0.45 μm and 0.22 μm mixed cellulose ester filter membranes (Millipore). After filtering, 2% (w/v) of activated charcoal (Sigma) was added to the solution and the mixture was agitated

for 1 hour at 250 rpm in an orbital shaker oven (IKA® KS 4000 ic control) at room temperature. Afterwards, the suspension was centrifuged at 60 000 ×g for 1 hour at 20ºC (Beckman Avanti J-26 XP, Beckman Coulter), the supernatant was carefully decanted and ultracentrifuged at 120 000 ×g for 1 hour at 20ºC (Beckman Optima L80-XP, Beckman Coulter). Finally, the supernatant was retrieved and filtered once more with 0.22 µm filter membranes, frozen at –20ºC, freeze-dried for 3 days (BenchTop Pro, VirTis) and stored at –20ºC until further use.

After the purification process was complete, pectin was functionalized by covalent grafting of the oligopeptidic sequence $(glycine)_4$-arginine-glycine-aspartic acid-serine-proline (G_4RGDSP, Genscript). The reaction was carried out by an adapted method of aqueous carbodiimide chemistry (**Figure 6**) [51, 62, 82]. Briefly, a 1% (w/v) solution of purified pectin was prepared in a 0.1 M 2-(*N*-morpholino) ethanesulfonic acid (MES) buffer solution (0.1 M MES buffering salt, 0.3 M NaCl, pH adjustment to 6 using a 1 M NaOH solution, Sigma) in ultrapure water. The solution was divided in two: the pectin to be functionalized (RGDpec) and the control (BLKpec). *N*-Hydroxy-sulfosuccinimide (sulfo-NHS, Aldrich) and 1-ethyl-(dimethylaminopropryl)-carbodiimide (EDC, Sigma, 59.65 mg per g pectin) at a molar ratio of 1:2 were added quickly and in this sequence to both solutions. The peptide was also rapidly added only to the RGDpec solution (50 mg per g pectin). The solutions were allowed to react for 20 hours at room temperature while stirring, and were then quenched with hydroxylamine hydrochloride (18 mg per g pectin, Sigma). Afterwards, both polymer solutions were dialyzed (MWCO 3500, Spectra/Por®, SpectrumLabs) against decreasing concentrations of NaCl solutions in deionized water (7.5 to 0 g/L) for 3 days, with solution renewal 3 times a day. Next, activated charcoal (2 wt%) was added to both solutions, they were stirred for 1 hour and ultracentrifuged twice as previously described. Once more, both solutions were filtered through 0.22 µm filter membranes (Steriflip® filter unit, Millipore), frozen, lyophilized and stored at –20ºC until further use.

The effectiveness of the RGD coupling to the purified pectin was assessed by a UV absorbance assay (200–260 nm region) against BLKpec using a 384-well UV transparent microplate (Greiner) in a micro-plate reader (PowerWave XS, BioTek). A calibration curve (**Annex I**) was prepared with a series of 1 wt % BLKpec with increasing RGD concentrations, which served as standard to determine the extent of the RGD grafting.

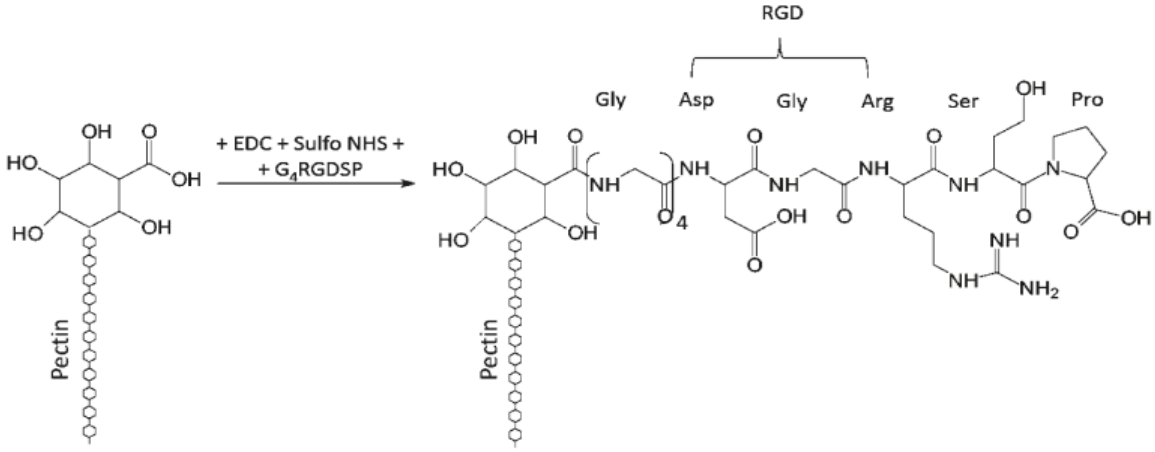

Figure 6 *– Schematic representation of pectin grafting with the RGD-containing peptide [Adapted from [62]).*

3.4 Preparation of hydrogel-bioactive glass composites

In situ crosslinking composite hydrogels were prepared adapting the internal gelation method described in the group's past studies that relies on the calcium carbonate/D-glucono-δ-lactone ($CaCO_3$/GDL) slow gelling system. In this method, GDL hydrolyses with time, lowering the pH of the mixture, which triggers the slow release of calcium from $CaCO_3$, promoting the formation of the egg-boxes, as previously described. To determine the quantities of both $CaCO_3$ and GDL, the stoichiometric ratio of Ca^{2+}-to-COO^- groups was determined according to **Eq. 1**, and the amount of GDL needed for the number of Ca^{2+} without severely affecting the pH of the solution was calculated using **Eq. 2** [51]. The COO^- groups of the pectin were estimated from its DM.

$$R = 2[Ca^{2+}]/[COO^-] \quad \textbf{(1)}$$

$$R_{Ca\text{-}GDL} = 2[Ca^{2+}]/[GDL] \quad \textbf{(2)}$$

In the present work, however, the calcium carbonate was completely replaced with the bioactive glass particles (both 1 μm and 8 μm) and gels were produced with and without GDL. For the preparation of hydrogels, 3% (w/v) pectin solutions were prepared in 0.9 wt % NaCl (VWR) in deionized water. Afterwards, an aqueous suspension of the

bioactive glass was carefully dispersed into the polymeric solution and either a freshly made GDL (Sigma) solution or its respective volume in 0.9 wt % NaCl was added to the mixture. The R and $R_{Ca\text{-}GDL}$ ratios were kept constant throughout the experimental work (R=1 and $R_{Ca\text{-}GDL}$=0.5, to ensure an excess of calcium, in order to increase the probability of saturating the egg-box zones) [51]. A set amount of the gel-precursor solution was transferred to a polytetrafluoroethylene (PTFE) surface inside a petri dish and compressed with another PTFE plate, and gel height was set using 1 mm spacers (**Figure 7**). The environment was kept humidified by adding deionized water to the bottom part of the petri dish and covering it, and the solutions were left to gel on their own for different amounts of time depending on their formulation.

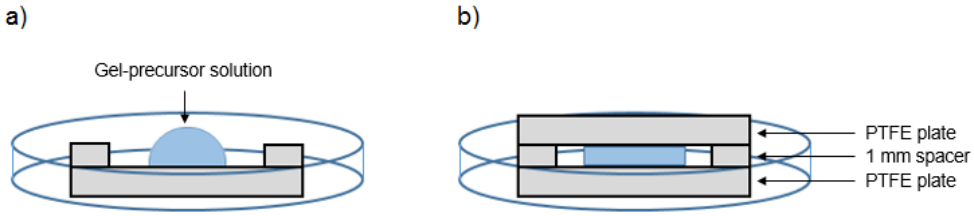

Figure 7 *– Hydrogel production scheme: a) Gel-precursor solution was pipetted into a PTFE plate; b) the gels were compressed with another PTFE plate and left to gel.*

Different hydrogel formulations were tested, varying Di-70 particle size, bioactive glass content and pectin concentrations. Those are described in **Table 6**. Only one formulation using GDL was tested.

Table 6 *– Tested hydrogel formulations.*

Formulation	Pectin % (w/v)	Di-70 φ (µm)	Di-70 Concentration (mg/mL)	GDL Concentration (mg/mL)
A	1.5	8	2.34*	-
B		1 and 8 (50% each)	2.34*	-
C		1	4.67	-
D			2.34*	-
E			1.17	-
F			2.34*	8.32
G	1		1.56*	-

*This bioactive glass content corresponds to the calcium carbonate concentration of the protocol for R=1 and $R_{Ca\text{-}GDL}$=0.5 and will hereafter be referred to as BG1. The other bioactive glass concentrations are either doubled (BG2) or halved (BG0.5).

3.5 Rheological characterization of the composite hydrogels

The rheological behaviour of the hydrogels and gel-precursor solutions was assessed using a Kinexus Pro rheometer (Malvern Instruments). Hydrogel disks were prepared from 40 µL of gel-precursor solution as previously described and incubated in 24-well plates at 37ºC. Initial tests were performed in gels that were incubated in 500 µL of water for 24 hours and, later on, some formulations were tested after incubation in 500 µL Dulbecco's modified eagle medium-Hepes (DMEM-HEPES, Gibco) for 1 and 3 days. For the selection of a formulation for further studies, the effect of adding 10% v/v fetal bovine serum (FBS, Gibco) to the medium was assessed.

The rheological tests were carried out at 37ºC in a water-vapour saturated environment ensured by the rheometer chamber. Gels were punched into cylinders (with 4 mm biopsy punch cylinders) and oscillatory measurements were performed using parallel plate geometries, compressing the gels by 20% of their height, iteratively performing frequency and amplitude sweep measurements in order to determine the gels' linear

viscoelastic region (LVR) (**Figure 8**). The viscoelastic properties of hydrogel solutions overtime were assessed using frequency and shear strain values within each formulation's LVR.

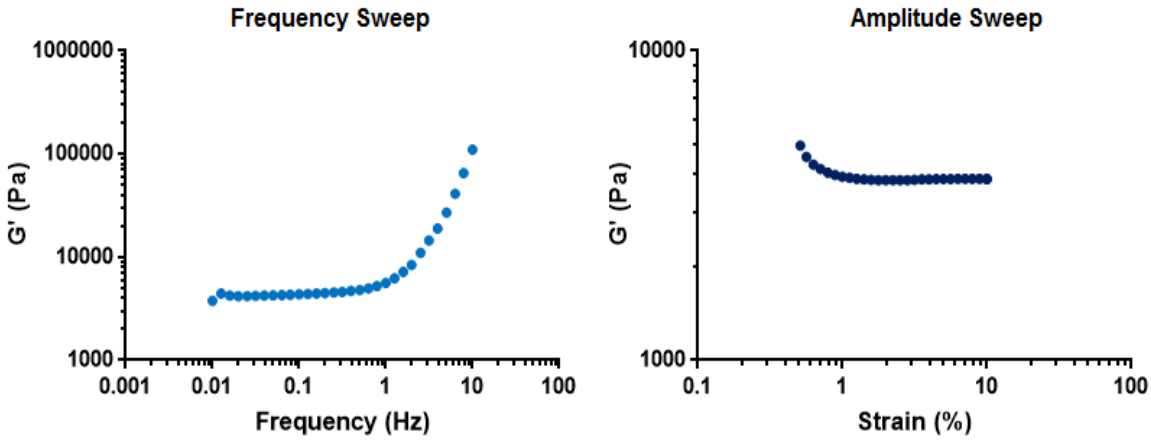

Figure 8 *– Examples of elastic component (G') of the shear modulus values obtained in frequency and amplitude sweeps for the determination of the LVR (D formulation after 24h incubation in DMEM-HEPES).*

3.6 Measurement of swelling profiles

To study the swelling profiles of the composite hydrogels, a final pectin concentration of 1.5% was set for five different formulations without GDL (formulations A through E, n = 4 for each formulation). Hydrogels prepared from 20 µL gel-precursor solution were produced as described in section **3.4**, and were incubated for 24 and 72 hours in 500 µL DMEM-HEPES at 37ºC. For each time point, gels were weighed (W1), frozen and freeze-dried. After the lyophilisation was complete, gels were weighed again (W2) and the swelling ratio (S_R) was calculated using the following equation:

$$S_R = W1 / W2 \quad \textbf{(3)}$$

3.7 *In vitro* stability studies

In order to assess the composite's stability in cell culture medium, 20 μL hydrogels (D formulation) were incubated in the same conditions later used for cell culture studies with mesenchymal stem cells, i.e., at 37ºC with minimum essential medium α (α-MEM, Gibco) supplemented with 10% v/v inactivated FBS and 1% v/v penicillin/streptomycin (P/S, Biowest) (complete α-MEM). Medium samples were retrieved after 1, 24 and 72 hours of incubation and complete medium that had not been in contact with the materials was used as a control. Samples were treated with 0.1% v/v nitric acid (65%, Merck) and stored at 4ºC until spectrophotometric analysis was performed to investigate the changes in medium composition. The investigated ions were the ones present in the bioactive glass composition (calcium, magnesium, silicon and phosphate), and absorbance values were measured. Calcium and magnesium were measured using flame atomic absorption spectroscopy (Perkin-Elmer, Aanalyst 200) and silicon and phosphate were measured using standard colorimetric methods with absorbance spectroscopy in the visible spectral region (Jenway 6100). Samples were read in triplicates and final concentration values were calculated with the aid of a calibration curve for each element (**Annex II**).

3.8 *In vitro* assessment of metabolic activity and cytotoxicity

In order to pre-screen metabolic activity and cytotoxicity of the hydrogel-bioactive glass composites prepared human dermal neonatal fibroblasts (hDNFs) isolated from foreskins of healthy male newborns (Zenbio) were used. hDNFs were cultured in DMEM supplemented with 10% v/v FBS (Gibco), 1% v/v P/S (Biowest) and 1% v/v amphotericin B (Capricorn Scientific) (complete DMEM). Cells were maintained at 37ºC in a humidified atmosphere of 5% CO_2 and at 80-90% confluence fibroblasts were trypsinized (0.05 wt% trypsin/EDTA solution). Cells from passage 6 were used in this study.

To determine the effect of the composite hydrogels, a cytotoxicity assay was performed using hDNFs according to ISO 10993-5 standard practice. For this test, cells were trypsinized at pre-confluence and centrifuged. After discarding the supernatant, 2×10^4 cells were seeded into 24-well plates and incubated in complete DMEM in a humidified

atmosphere of 5% CO_2 at 37ºC. Simultaneously, 20 µL hydrogels (D formulation – 1.5% pectin, 1 µm glass particles, BG1 content) were incubated under the same conditions. After 24 hours of incubation, both a direct contact and indirect contact test were performed (n=3). For the direct contact assay, samples were directly put into the wells containing fibroblasts and the medium was refreshed. For the indirect contact assay, the medium was replaced by the medium that had been incubated with the hydrogels for 24 hours. As a control, wells with fibroblasts that were not in contact with the materials were used. The results were obtained through a resazurin-based assay. Briefly, culture medium was removed and replaced with 500 µL complete medium with 20% v/v resazurin (Sigma) and the 24-well plates were incubated for two hours at 37ºC in a humidified incubator with 5% CO_2. Then, 100 µL from each well were transferred to wells of a black 96-well plate and fluorescence was measured (λ_{ex} = 530 nm, λ_{em} = 590 nm) using a micro-plate reader (Synergy MX, BioTek).

For the pre-screening of cell entrapment, hDNFs were loaded within composite hydrogels. hDNFs were trypsinized before reaching confluence and centrifuged. The supernatant was discarded, cells were carefully added to the gel-precursor solution (10^7 cells/mL) and gels were produced from 20 µL of this solution, as previously described. For completion of gelling, samples were placed in an incubator (37ºC, 5% CO_2 humidified atmosphere) for about 1 hour. After that, gels were placed in 24-well plates and complete DMEM was added. After 24 hours, the culture medium was replaced once more. At days 1 and 7 of culture, cell metabolic activity was measured as described in the section below. For this assay, two hydrogel formulations were produced (C and D, both having a final pectin concentration of 1.5% and 1 µm glass particles, but with different Di-70 contents, BG2 and BG1 respectively). Two different pectins were also tested: RGDpec (with a final RGD density of 200 µM) and BLKpec as a control. Cell metabolic activity at different timepoints was evaluated using a resazurin-based assay as previously described.

Cell morphology was investigated for entrapped hDNFs after 1 and 7 days. Fibroblast-loaded hydrogels were washed with phosphate-buffered saline (PBS), fixed for 20 minutes in 4% PFA/PBS and stained for filamentous actin (F-actin) and nuclei. Briefly, after fixation and rinsing, samples were permeabilized with 0.1% Triton X-100 (Sigma) in PBS for 5 minutes. They were then incubated for 30 minutes with 1% bovine serum albumin (BSA, Merck) in PBS. For F-actin staining, samples were incubated with the

conjugated probe phalloidin/alexa fluor® 488 (Molecular Probes-Invitrogen, 1:40 in 1% BSA) for 1 hour at room temperature. Finally, samples were washed three times with PBS and nuclei were counterstained with 4',6-diamidino-2-phenylindole dihydrochloride (DAPI, H-1200, Vector) just before confocal visualization (CLSM, Leica SP2AOBS, Leica Microsystems) using LCS software (Leica Microsystems). The scanned Z-series were projected onto a single plane and pseudo-coloured using ImageJ.

3.9 Biological behaviour of mesenchymal stem cells embedded within composites

The biological behaviour of the prepared composites was assessed using embedded therapeutically relevant cells for orthopaedic applications. Human mesenchymal stem cells (hMSCs) isolated from bone marrow (Lonza) were cultured in α-MEM supplemented with 10% v/v inactivated FBS (Gibco) and 1% v/v P/S (Biowest) (complete α-MEM) at 37ºC in a humidified atmosphere of CO_2. Cell culture medium was changed every 2–3 days, and cells were trypsinized (TrypLE™) at pre-confluence. For this study, cells were used in passage 12.

The production of cell-embedded gels with hMSCs was similar to the procedure described for fibroblast entrapment, although cell density used in the present case was 8×10^6 cells/mL and complete α-MEM was used instead of DMEM. The medium was changed every 2–3 days. To induce the differentiation of hMSCs along the osteoblastic lineage, hydrogels were also incubated with osteogenic medium: basal medium supplemented with 100 nM dexamethasone (Sigma-Aldrich), 10 mM β-glycerophosphate (Sigma-Aldrich) and 0.05 mM 2-phospho-L-ascorbic acid (Fluka). Cell-laden hydrogels were kept in culture for up to 21 days and a single formulation was tested (D), both with RGDpec and BLKpec as described above. 20 µL samples were used to assess cell metabolic activity, morphology and differentiation and 40 µL samples were used to evaluate their rheological properties. Rheological analysis of composites with embedded cells was performed in samples after 1 and 14 days in culture using both basal and osteogenic media. Shear moduli component values were averaged from amplitude and frequency sweeps within the LVR.

To assess the differentiation of hMSCs embedded into the composite, a Von Kossa staining assay was performed. Samples from days 7 and 21 of culture were washed in Tris-buffered saline (TBS) and cells were fixed with 4% PFA/TBS for 20 minutes. Afterwards, samples were incubated for 30 minutes under UV light in 500 µL of a 2.5% (w/v) silver nitrate solution. Then, the materials were rinsed with deionized water and incubated in 500 µL of sodium thiosulfate 5% (w/v) for 3 minutes at room temperature. After rinsing with deionized water once more, samples were observed under a stereomicroscope (Olympus SZX9).

Cell morphology was also investigated for hMSCs (time-points: day 1 and 21). Mesenchymal stem cell-loaded hydrogels were washed with TBS, fixed in 4% PFA/TBS, and finally stained for filamentous actin and nuclei, similarly to the procedure previously described, but using TBS instead of PBS. The visualization and image processing procedures were performed as described in section **3.8**.

3.10 Statistical analysis

Statistical analyses were performed using GraphPad Prism 7.02 software. Data was analysed using the non-parametric Mann–Whitney test. All tests were performed using a 95% confidence interval and statistically significant differences are marked with either different symbols between parameters or with a * ($p < 0.05$). Some statistical data is presented in **Annexes III** and **IV** in table format in order to increase correspondent figure readability.

– This page was intentionally left blank –

Chapter 4

Results and Discussion

4.1 Bioactive glass characterization

4.1.1 Crystallographic characterization

The X-ray diffraction spectrum of the bioactive glass frits is presented in **Figure 9**. It was possible to confirm the amorphous structure of the glass due to the absence of crystalline phases.

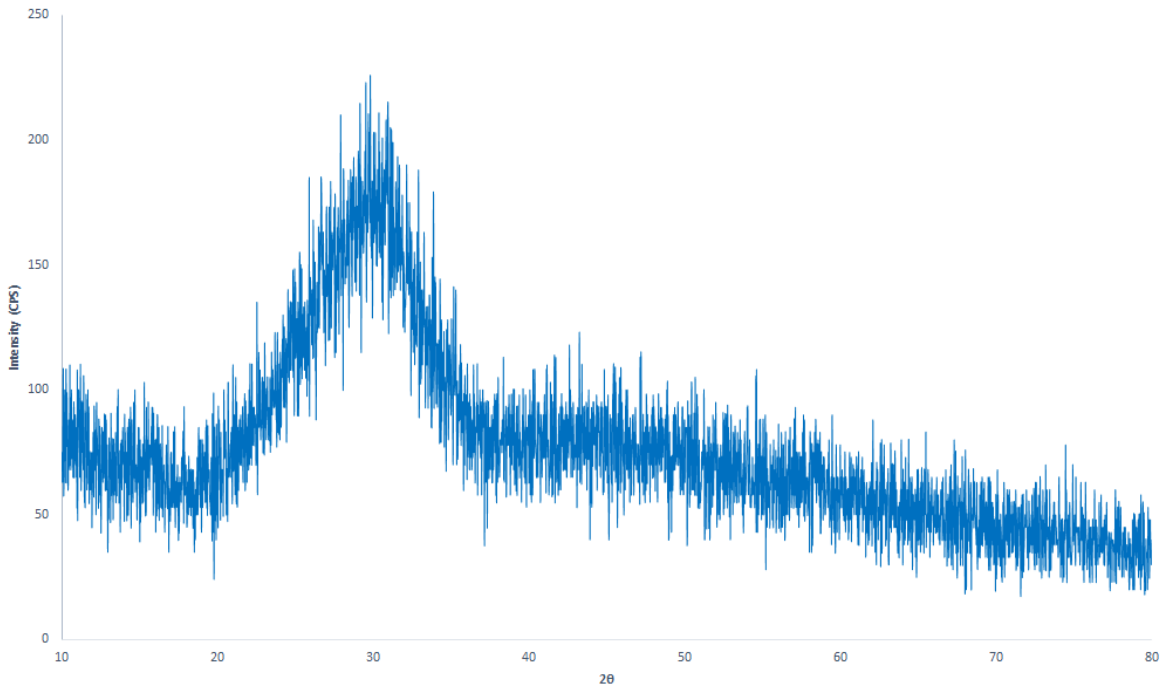

Figure 9 *– XRD spectrum of the Di-70 glass frits.*

4.1.2 Particle size distribution

Given that the particle size of the reinforcing component (bioactive glass) greatly influences the composite's mechanical and biological properties [72-74], and since the study of those effects was one of the objectives of this work, bioactive glass particle size distribution was assessed. As previously described, after drying the glass frits, they were submitted to a planetary milling process, which allowed obtaining particles with a mean size of approximately 8 µm. Afterwards, in order to achieve smaller particle sizes, glass powder was wet milled for several hours, and the evolution of the process is showed in **Figure 10**.

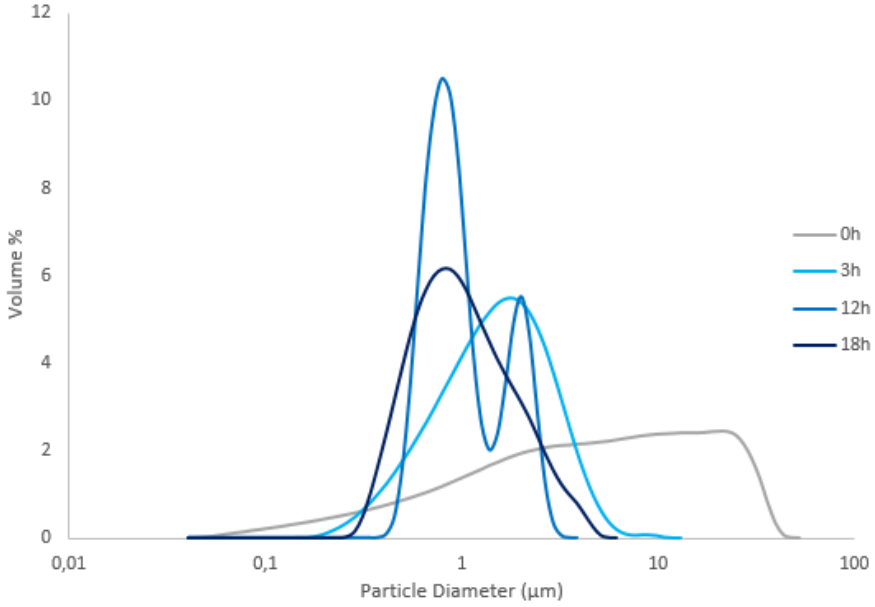

Figure 10 *– Bioactive glass particle size evolution throughout the wet ball milling process. The 0h line corresponds to particle size distribution after the planetary milling process for 2 hours.*

After just 3 hours of wet milling, mean particle size was decreased to 1.8 µm and after 12 hours particle mean size reached 1.2 µm. However, the particle size distribution graph in **Figure 10** indicates that, even though mean particle size was 1.2 µm, particles were not evenly distributed, possibly due to aggregation, despite the fact that light scattering tests were performed after ultrasonic agitation and using a dispersant (Targon 1128) to reduce attraction forces between the particles [83]. However, increasing mill time to 18 hours allowed the obtention of evenly distributed particles, whose mean size was approximately the desired 1 µm.

4.2 Pectin characterization

Plant-extracted polymers usually have some content of contaminants such as proteins, polyphenols and endotoxins, which is why a purification process is necessary before preparing a material for biomedical applications. Despite its great interest for tissue engineering applications, pectin is not commercially available in medical grade purity. Previous studies from the group report that a purification protocol close to the one used in this work lead to a 70% decrease in protein content, 52% in polyphenols content and 96% in endotoxin levels [51]. The efficiency of the purification method used in this work was calculated taking into consideration the initial mass of raw pectin and the final mass of purified pectin, and resulted in a yield of 71%.

After purification, pectin was functionalized with an RGD containing peptide and the UV spectrum of RGDpec showed the presence of a characteristic peak around 230 nm, which indicated effective peptide grafting to the polymer. With the aid of a calibration curve (**Annex I**) produced from the analysis of several spectra of pectin solutions containing different known RGD concentrations (**Figure 11**), the quantity of RGD successfully grafted into the polymer was estimated to be of 22 mg per g of pectin.

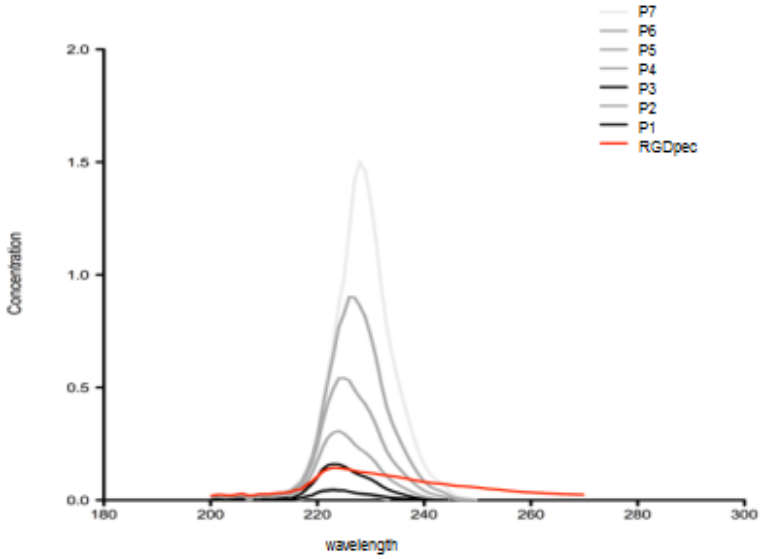

Figure 11 *– UV spectrum of RGDpec and Blank pectin solutions containing different RGD concentrations.*

4.3 Physico-chemical characterization of composites

4.3.1 Rheological characterization

Initial rheological tests were performed to samples incubated in water for 24 hours at 37 ºC to provide a preliminary evaluation of the materials properties and their gelation profiles. Five formulations containing the standard BG1 glass concentration were tested: A, B, D, F and G. The first four samples correspond to 1.5% pectin gels, being A with 8 µm glass particles, B with a mixture of 8 and 1 µm particles, D with 1 µm particles without GDL, F being similar to D but using GDL, and finally G being similar to D with a lower pectin concentration (1%).

The linear viscoelastic region for each formulation was determined, shear moduli components values were obtained (**Figure 12**) and gelation tests were performed (**Table 7**). The gelation profile of hydrogels was used to evaluate the time necessary for gels to present a solid-like behaviour. Gelation was considered to be triggered when there was a crossover between the elastic (G') and viscous (G'') components of the shear modulus (i.e., the time at which the phase angle, δ, goes below 45º), and it was decided that gels exhibited a solid-like behaviour when the phase angle went below 10º [51] (**Figure 13**).

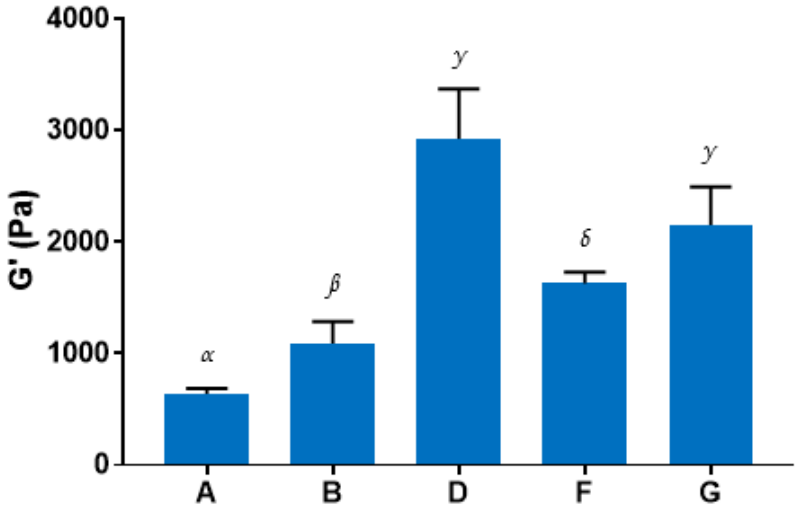

Figure 12 *– Shear modulus - elastic component (G') - values for the preliminary scanning of the different composite formulations in water (37ºC). Different symbols denote statistically significant differences between G' values of different formulations ($p<0.05$, $n=4$).*

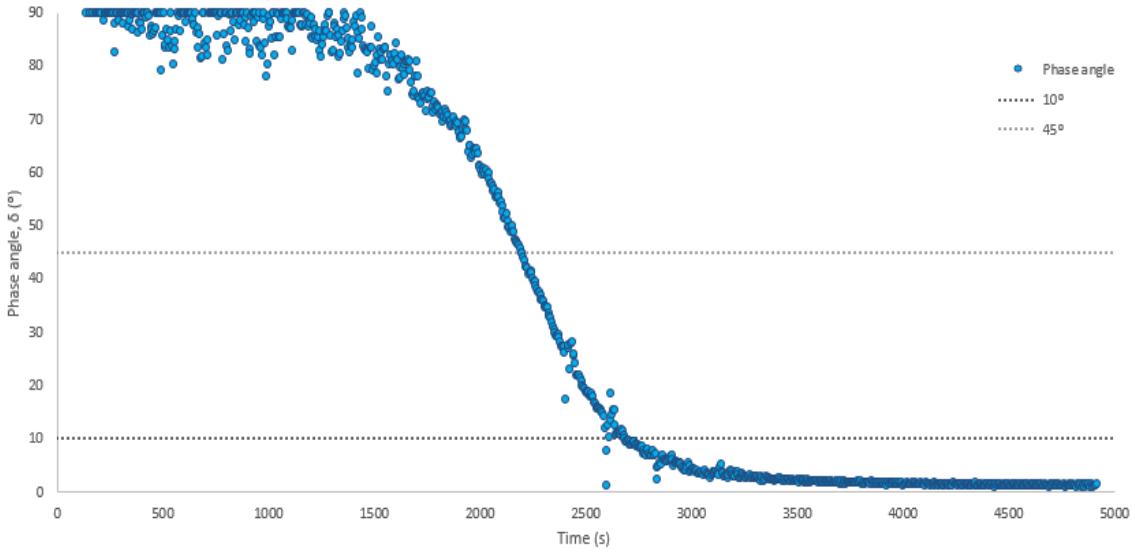

Figure 13 *– Gelation test performed to sample of formulation D. Phase angle dropped below 45º after approximately 25 minutes, and below 10º after 30 minutes. The test was carried at constant 0.1 Hz and with 1% constant strain (LVR).*

Table 7 *– Gelation profiles of the composites.*

Formulation	Gelation triggering time (δ <45º) (min)	Solid-like behaviour (δ <10º) (min)
A	80	95
B	33	40
D	25	30
F	1	1.5
G	35	40

Rheological analysis revealed that the bioactive glass-reinforced pectin-based composites prepared are able to form hydrogels without adding GDL for pectin crosslinking, within clinically relevant time frames. The addition of GDL creates an

additional unnecessary stress for cells when their entrapment is envisioned due to its pH lowering effect, and increases hydrogel production complexity [6].

Rheometry results showed that composites with finer glass particles had higher shear modulus values and lower gelation times. A, B and D formulations differ only in glass particle size, and D (with only 1 μm particles) clearly showed higher G' values. As polymer concentration decreased to 1% (formulation G, which had the same glass concentration and particle size as D), an evident decrease in elastic component value was observed, as well as a slight increase in gelation times. Neves *et al.* (2015) reported similar results, where 1.5% pectin hydrogels produced by internal gelation presented lower G' values and longer gelation times when compared to 2.5% pectin hydrogels [51].

Regarding gelation times, formulation A took the longest time to stiffen, and this formulation was discarded from further tests since 95 minutes for gelation was considered an inadequate amount of time for cell survival in a potential embedding process. The addition of GDL (formulation F) proved to hasten the gelation, although its shear modulus values varied too quickly, which could also lead to increased cell stress. Since it was shown that these composites can form hydrogels without GDL within clinically acceptable timeframes, this component was not included in further tests.

The effect of bioactive glass concentration was also assessed. Formulations C and E (BG2 and BG0.5 concentrations, respectively) were compared to the previously analysed formulation D (BG1 concentration). For these tests, instead of using water, samples were incubated in DMEM-HEPES at 37ºC to provide more meaningful biological significance, and rheological tests were performed after 1 and 3 days of incubation to evaluate the material's properties overtime (**Figure 14**).

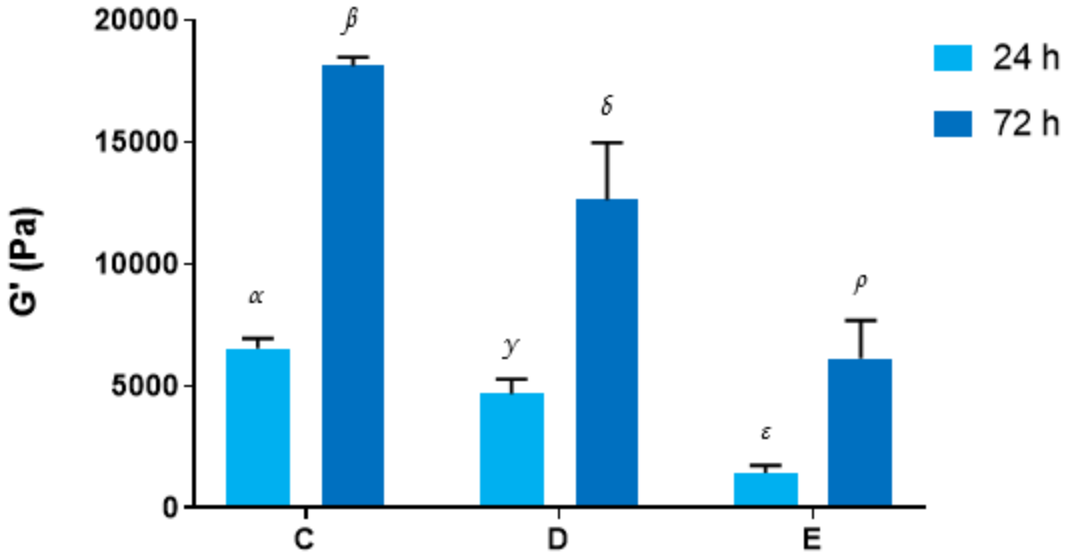

Figure 14 *– Shear modulus - elastic component (G') - values of formulations varying in Di-70 content after incubation at 37ºC in DMEM-HEPES for up to 3 days (pectin concentration kept constant at 1.5% and glass particle size of 1 μm). Different symbols denote statistically significant differences between G' values of different formulations and timepoints ($p<0.05$, $n=4$).*

Results from **Figure 14** show that the reinforcement content also had a significant effect in the composite's properties. The incubation medium influenced the properties of the hydrogels since, after 24 hours, D samples incubated in DMEM-HEPES exhibited a much higher G' value than comparable samples incubated in water (4590 Pa in DMEM-HEPES vs. 2950 Pa in water). It is also shown that shear modulus values also tend to increase with time, as evidenced for every tested formulation. These effects could be related to the presence of calcium in the medium's composition (under the form of calcium chloride, according to the manufacturer), which could potentiate the crosslinking of pectin overtime. As expected, higher glass concentrations also translated into higher G' values due to higher cation content. Gelation times were also affected by the presence of different quantities of Di-70, as gels took longer to form with lower glass concentrations (C: $t_{\delta<45^o}$=20 min, $t_{\delta<10^o}$=25 min; D: $t_{\delta<45^o}$=25 min, $t_{\delta<10^o}$=30 min; E: $t_{\delta<45^o}$=75 min, $t_{\delta<10^o}$=105 min). The E formulation, which had the lowest amount of bioactive glass (BG0.5), and similarly to the previously analysed formulation A, presented a very long gelation time, unsuitable for the embedding of cells. Formulation C, although with a similar gelation time to D, displayed a much higher variation in G' values overtime, which could also inhibit maintenance of cell viability due to impacts on their ability to adhere and proliferate [84].

Hence, formulation D yielded the most appealing properties in terms of shear modulus values and gelation times and, as such, an additional rheological characterization assay was performed in order to evaluate the effects of adding FBS to the incubation medium (**Figure 15**). LVR studies were once more carried out for D samples that had been incubated for 1 and 3 days at 37ºC, this time in DMEM-HEPES supplemented with 10% v/v FBS. These results showed an increase in G' values after both 24 and 72 hours, even though differences weren't statistically significant at day 3. This effect could once more be related to the presence of additional crosslinking agents in the medium influenced by the FBS, as Vetsch *et al.* (2015) reported the appearance of calcium deposits on the surface of scaffolds cultured with some types of serum, even in acellular conditions [85].

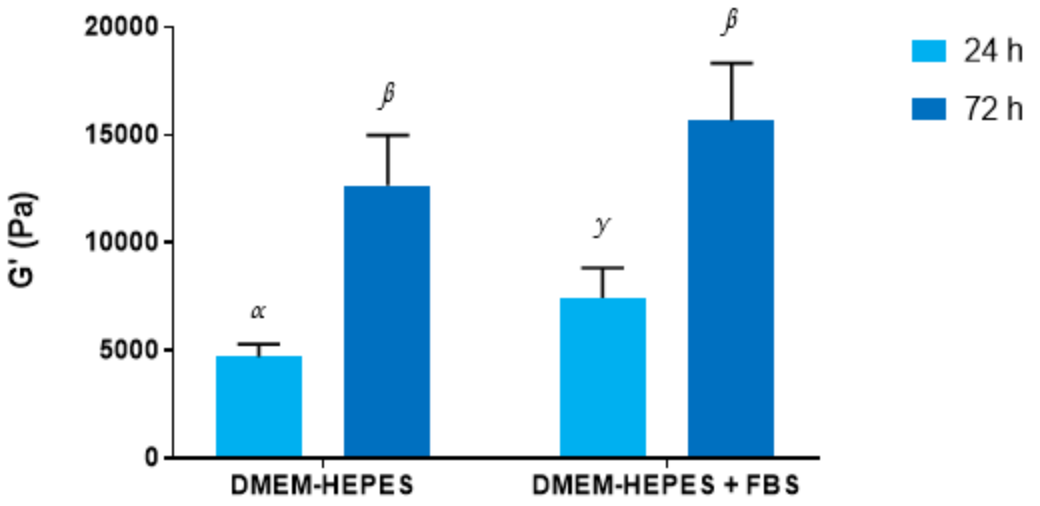

Figure 15 *– Shear modulus - elastic component (G') - values of formulation D hydrogels incubated with and without 10% FBS at 37ºC for up to 3. Different symbols denote statistically significant differences between G' values of samples from different incubation media and timepoints ($p<0.05$, $n=4$).*

4.3.2 Swelling profiles

For the study of the swelling profiles of the hydrogel composites, formulations containing a constant pectin concentration of 1.5% and variable glass content in terms of concentration and particle size (formulations A, B, C, D and E) were incubated in DMEM-HEPES for up to 72 hours (**Figure 16**).

From the analysis of **Figure 16**, it is possible to infer that the first 24 hours were the most important for the swelling of composites. In these first 24 hours, formulations containing only finer glass particles (D and E) showed similar and higher swelling ratios when compared to the other formulations. However, the swelling ratio of formulation D remained stable between 24 and 72 hours, while the swelling ratio of formulation E decreased with time. This makes Formulation D more attractive for cell entrapment, since it provides a more stable environment for cell proliferation sooner than other compositions. Formulation C, even though it was also produced with 1 µm glass particles, presented very different results, having the lowest ratio at 24 hours and the highest after 72 hours, suggesting that a higher glass content (BG2) significantly interferes with the hydrogel matrix. This was an unexpected result, as literature suggests that higher glass contents result in lower swelling percentages and water uptakes due to the glass particles occupying the free voids within the polymeric matrix [65, 70]. It should also be noted that even after 72 hours, formulation C still had not achieved swelling equilibrium.

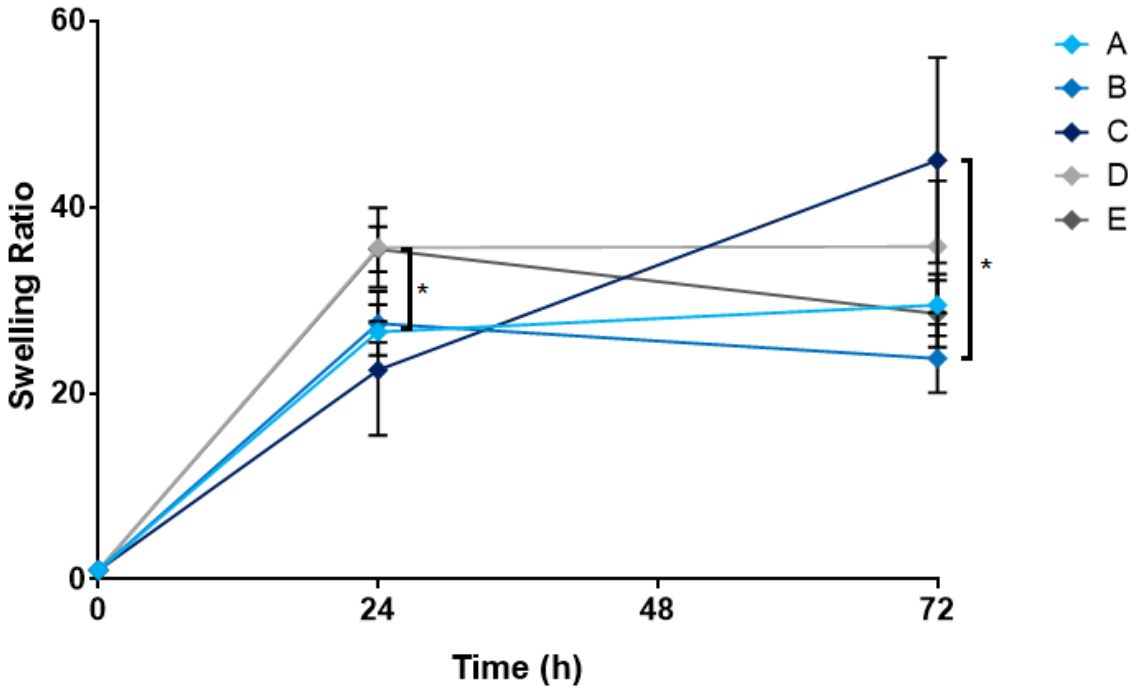

Figure 16 *– Swelling profiles of A, B, C, D and E formulations of composites. Higher bioactive glass content (C) translated in a higher swelling ratio with time. Mixture of two particle sizes seems to significantly change the swelling profile of the hydrogels. Legend: * mark denotes statistically significant differences between swelling ratios of different formulations and timepoints ($p<0.05$, $n=4$).*

Gels containing 8 μm glass particles (A and B) presented similar swelling ratios at time-point 24 hours, yet their behaviour changed with increasing incubation time. After incubation for 72 hours, the hydrogel with mixed glass particle sizes (B) seemed to retract the most out of the studied samples, having the lowest swelling ratio at that time-point. Comparing formulations A and D, which contained similar glass content but 8 μm and 1 μm glass particles respectively, exhibited expected swelling profiles, with composites with finer glass particles presenting higher swelling ratios, which could be related to the higher surface area and higher extent of exposure of the 1 μm particles on the material's surface [73].

Retrieving samples from an earlier timepoint than 24 hour time period could be interesting in future work in order to understand what happens in the first few moments of immersion and when the most critical alterations occur. Longer incubation times could also provide relevant information regarding equilibrium swelling rates.

One additional detail that was noticeable for formulation C was that after 72h in DMEM-HEPES, some turbidity was detected, which could be related to an initial diffusion of excess glass particles into the medium followed by some kind of precipitation. For that reason, changes to the medium's composition were analysed.

4.3.3 *In vitro* stability in cell culture medium

In order to analyse the stability of the prepared composites in cell culture medium, changes in cell culture medium induced by the presence of the composites were assessed. Composites (D formulation) were incubated in complete α-MEM and the concentration of ions in the medium was assessed over time, as presented in **Figure 17**.

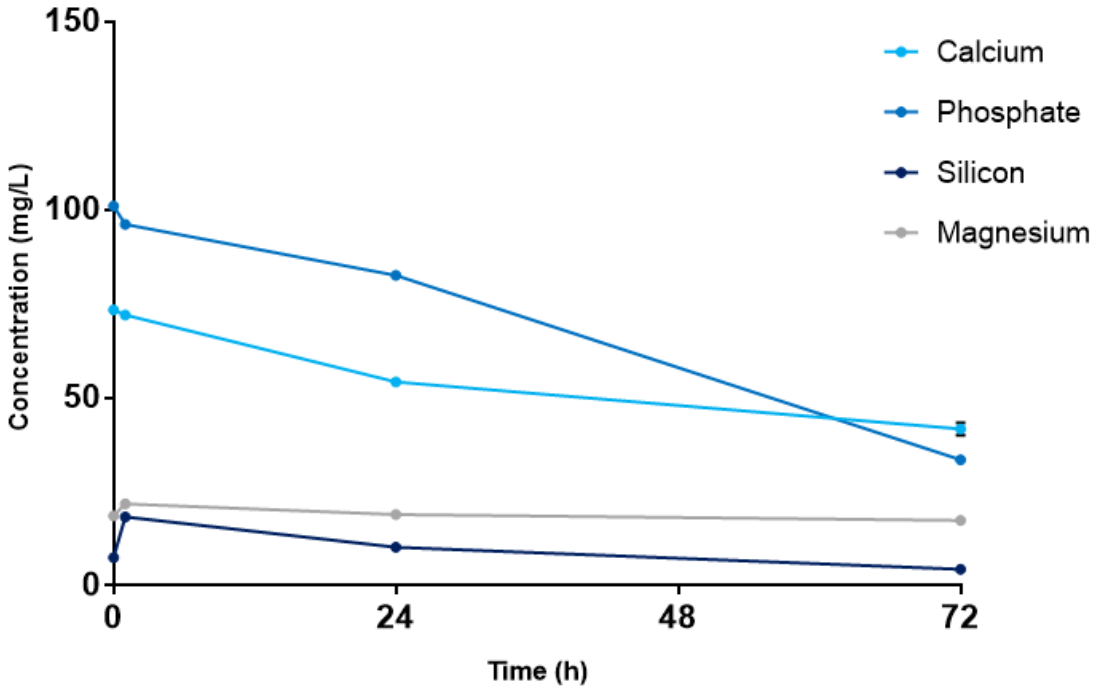

Figure 17 *– Alterations in concentration of bioactive glass components in cell culture medium after 1, 24 and 72 hours immersion of composites.*

Analysis of **Figure 17** indicates that the composites had, indeed, influence in the chemical stability of cell culture medium. **Figures 17** shows a decrease in medium concentration of calcium and phosphate (as determined by spectrophotometric analysis) which may be related to the formation of calcium phosphate (such as hydroxyapatite) deposits on the material, and which could be further investigated with surface or bulk analysis of the material (for instance, XRD and Fourier transform infrared spectroscopy (FTIR) analysis) [69, 73]. Additionally, calcium concentration could be decreasing due to further reticulation of pectin, congruent with the increase of G' values of gels incubated in cell culture medium.

For the remaining ions (silicon and magnesium), a clear increase in both elements' concentrations was noticeable in the first hour of contact with the samples, which may be due to the initial dissolution of these components into the medium, considering Di-70's high content of both SiO_2 and MgO. However, in the following 24 hours these medium concentrations started to decrease, possibly due to a recrystallization of the particles. Magnesium's levels tended to stabilize to initial values, but silicon content dropped below the initial medium concentrations, which is in agreement with Hench's model for *in vitro*

effects of bioactive materials, due to the establishment of a silicon-rich layer at the material's surface [45, 47]. Further studies on this topic could help better characterize the composite's effect on cell culture medium and how it influences cell growth, proliferation and viability.

4.4 *In vitro* assessment of metabolic activity and cytotoxicity

The cytotoxicity of the composite hydrogels was evaluated using direct and indirect contact tests, according to ISO 10993-5 standard practice. Formulation D was the one selected for this assay due to the previously presented favourable characteristics, namely its more stable rheological properties and swelling profile, as well as interesting *in vitro* effect on cell culture medium, making it suitable for tests with cells. Indeed, the materials were proved to be non-cytotoxic to cultured fibroblasts, as both direct and indirect contact assay results showed cell metabolic activity values above 70% of the controls' measured values (**Figure 18**).

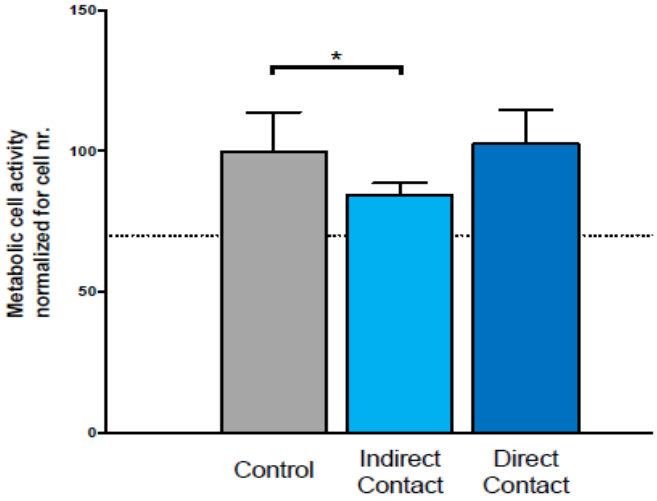

Figure 18 *– Metabolic cell activity normalized for cell number for each assay of the cytotoxicity test. Both Indirect contact and direct contact tests show positive results. Legend: * mark denotes statistically significant differences between measured metabolic activity of tests comparing to the control ($p<0.05$, $n=3$).*

The positive results of this initial scanning assay allowed the next step of the work to be performed consisting in the embedding of cells into the composite's matrix, which increases the material's likelihood of being used as a cell delivery system in tissue

engineering and regenerative medicine applications. At this stage of the work, fibroblasts were used instead of mesenchymal stem cells due to being easier to culture and having higher proliferative rates, making them more appropriate for the pre-screening and optimization processes.

Cell metabolic activity of the hDNFs embedded within the composite matrices was measured after 1 and 7 days in culture with a resazurin assay (**Figure 19**). Formulations C and D were tested in this assay, as well as both BLKpec and RGDpec. Statistical analysis results can be found on **Annex III**.

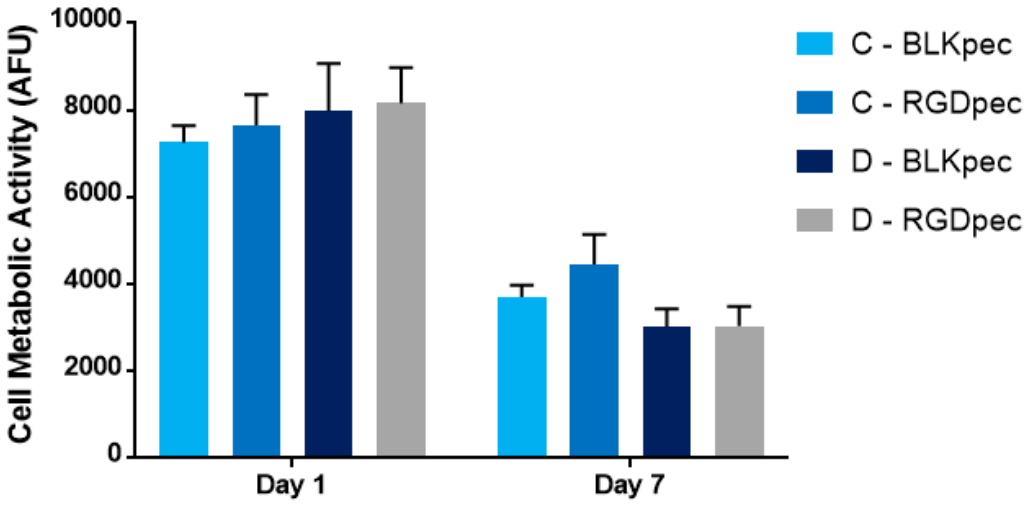

Figure 19 *– Metabolic activity of hDNFs embedded in composite hydrogels (formulations C and D, both with BLKpec and RGDpec) after 1 and 7 days of culture. Statistical analyses were performed to compare each formulation through every time-point and different formulations within the same time-point.*

At day 1 of culture, no statistically significant differences could be noted between the formulations, although both BLKpec and RGDpec of formulation D showed higher values than those of formulations C. At day 7, however still metabolically active, cells embedded in all different composites exhibited lower metabolic activity values comparing to day 1. This behaviour has already been reported for hydrogels containing embedded fibroblasts and it was linked to the contraction of the hydrogel's matrix after long culture time periods [86]. Moreover, this decrease in metabolic activity could be associated with the composite's released ions, although additional studies on this topic would be required in order to confirm if their effect is indeed detrimental for fibroblast viability. Nonetheless, RGDpec displayed better results than BLKpec, as expected due to the peptide's ability to

promote cell anchorage and the establishment of inter-cellular networks [51]. This was particularly notable in formulation C's results, which presented statistically significant differences between BLKpec and RGDpec at day 7.

The morphology of embedded hDNFs was assessed by labelling their actin filaments and nuclei and analysing by confocal microscopy. Samples were washed and fixed using PBS, which degraded the hydrogels containing lower bioactive glass concentrations, that being the reason why only projections of C formulations are presented in **Figure 20**.

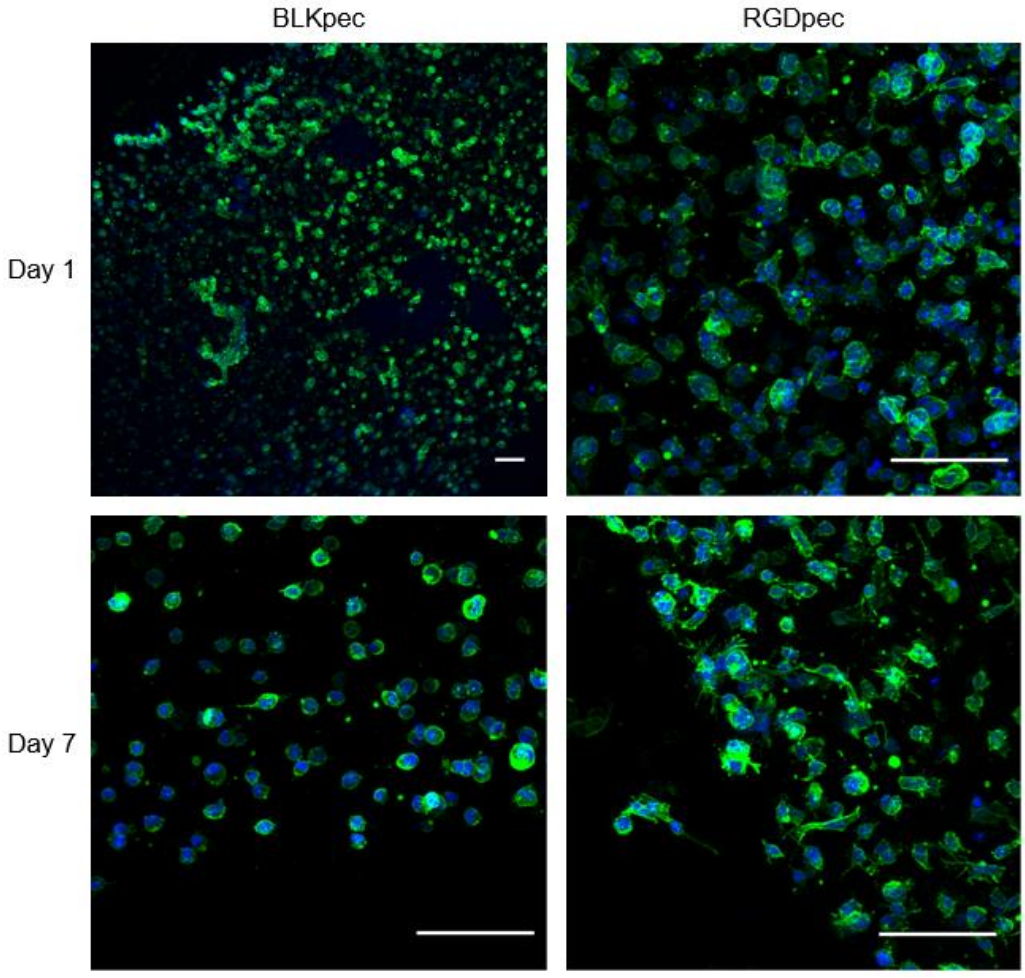

Figure 20 *– Morphology and spatial arrangement of human dermal neonatal fibroblasts embedded within composite hydrogels (C formulation) after 1 and 7 days of culture, stained for F-actin (green) and nuclei (blue) (scale bars: 100 μm).*

Depending on the matrix in which they were embedded, fibroblasts presented different morphologies and spatial organisation. A great difference is noticeable after 7 days in culture, where RGDpec provided a matrix suitable for cell spreading, as it is

possible to see cell-to-cell contact points. On the contrary, cells embedded in BLKpec presented a round shape, which is not typical for fibroblasts. Another interesting observation is that, in RGDpec, dividing cells can be observed, proving that even though they were exposed to high stiffness values, the composite mesh allowed fibroblasts to grow and proliferate.

4.5 Biological behaviour of mesenchymal stem cells embedded within composites

After the pre-screening and optimization processes, further tests were carried out using therapeutically relevant cells for orthopaedic applications, i.e. mesenchymal stem cells, with the selected formulation D composites, due to their previously proved interesting mechanical and biological properties. Cell metabolic activity of the hMSCs embedded within the composite matrices was measured after 1, 14 and 21 days in culture under basal and osteogenic conditions with a resazurin assay (**Figure 21**). Hydrogels using D formulation were tested in this assay, as well as both BLKpec and RGDpec. Statistical analysis results can be found on **Annex IV**.

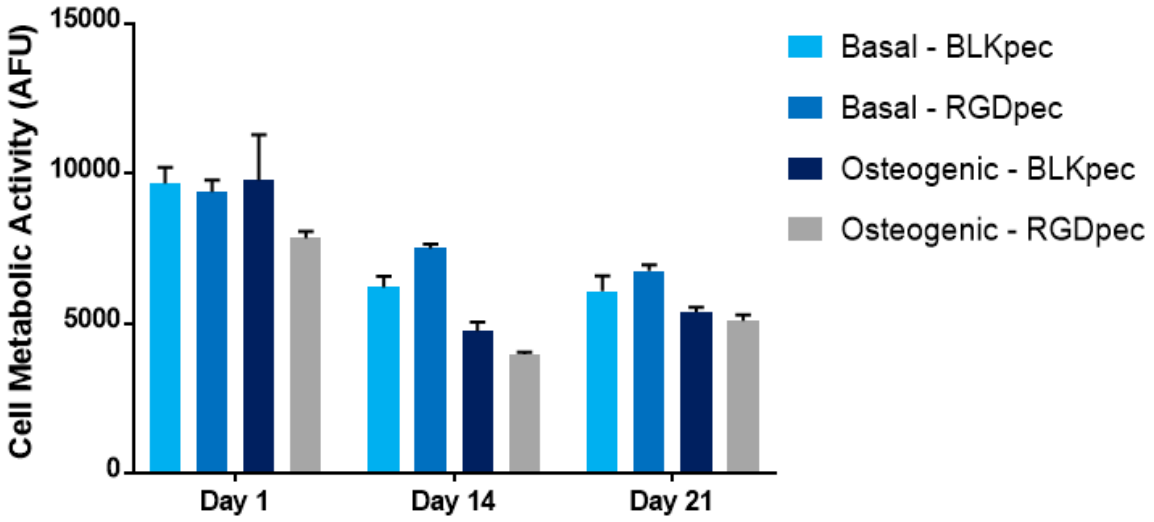

Figure 21 *– Metabolic activity of hMSCs embedded in composite hydrogels (Formulation D, both with BLKpec and RGDpec) after 1, 14 and 21 days of culture in basal or osteogenic medium. Statistical analyses were performed to compare each formulation through every time-point and different formulations within the same time-point.*

The graph in **Figure 21** shows that a slight decrease in metabolic activity was observed throughout the whole experience for all samples, similarly to what happened with the fibroblast-laden hydrogels. In this case, however, the decrease was much less significant. At day 1, every sample presented similar results with the exception of cells in composites produced with RGDpec and cultured under osteogenic conditions, which showed slightly lower values. At day 14, all four conditions presented a slight decrease in cell metabolic activity, with formulations using BLKpec not exhibiting statistically significant differences. Additionally, metabolic activity for cells in basal medium was noticeably higher than that of cells in osteogenic medium. After 21 days in culture, while metabolic activity for cells under basal conditions mostly remained stable and higher than in osteogenic conditions, there was a small increase in hMSCs' activity in an osteogenic medium. Overall, cells remained viable during the full duration of the assay and their metabolic activity was slightly higher for the basal media conditions. Previous studies testing the viability and differentiation of hMSCs seeded on the bioactive glass used in this work (Di-70) showed similar metabolic activity results to the ones obtained here, with cells under basal conditions presenting higher fluorescence values than those cultured in osteogenic medium at 14 days of culture [49]. Nonetheless, this composite provided a favourable environment to maintain cell viability without the need to add osteogenic supplements, possibly due to the release of ions that influence cell behaviour. Indeed, it has been reported that the ionic products of the dissolution of Si-, Ca- and Mg-containing bioactive ceramics could stimulate the growth, proliferation and osteogenic differentiation of mesenchymal stem cells [49, 87].

The morphology and organisation of hMSCs embedded within the hydrogels was assessed by labelling their actin filaments and nuclei and analysed by confocal microscopy. Data from day 21 of cell culture in both basal and osteogenic medium are shown in **Figure 22**.

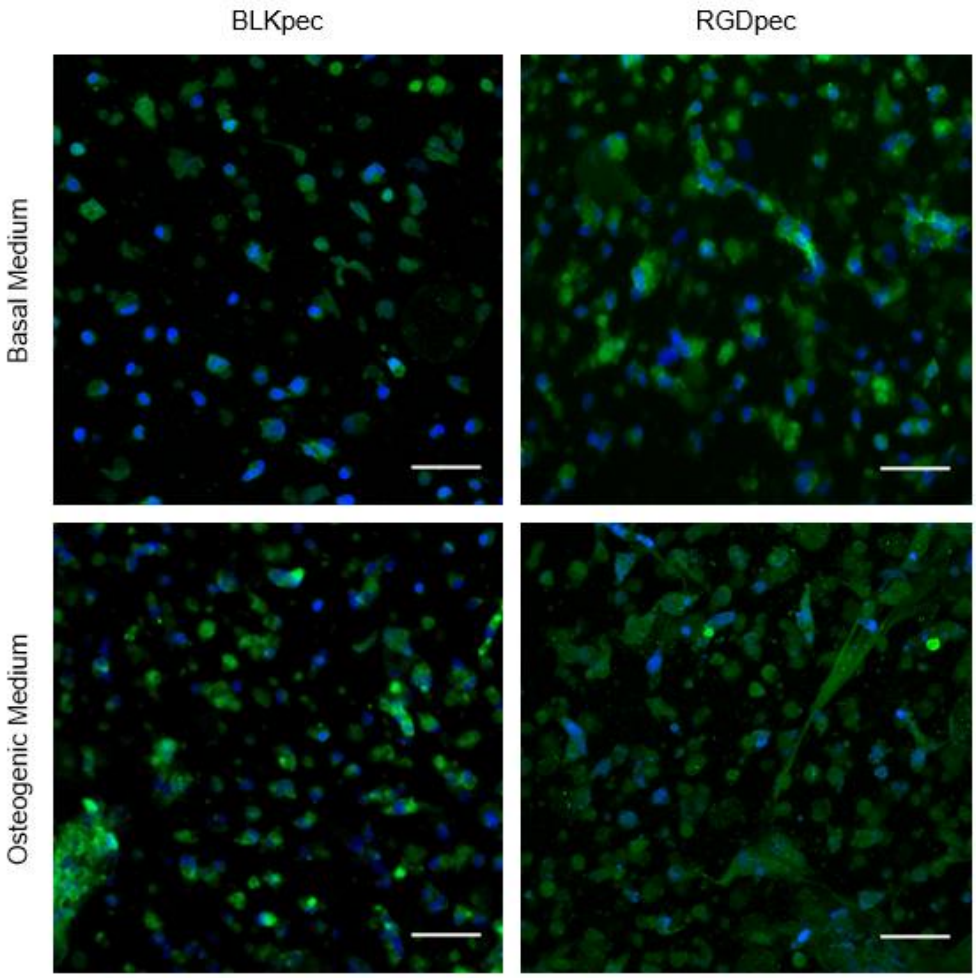

Figure 22 *– Morphology and spatial arrangement of human mesenchymal stem cells embedded within composite hydrogels (D formulation) after 21 days of culture in basal or osteogenic medium, stained for F-actin (green) and nuclei (blue) (scale bars: 60 μm).*

From the analysis of **Figure 22**, it can be inferred that, similarly to the results obtained for the hydrogels containing fibroblasts (**Figure 20**), RGDpec provided an environment apparently more suitable for cell spreading and proliferation. Indeed, cells observed in gels prepared with BLKpec appear round-shaped whilst the ones in RGDpec hydrogels were able to spread and establish contact points between each other. Other studies that compared the morphology of hMSCs embedded into BLKpec and RGDpec hydrogels showed similar results, with clear differences between formulations at 14 days of culture [51]. Additionally, the mechanical properties of the materials also differ substantially (results presented below), with the present composite hydrogels displaying higher shear modulus elastic component values, which could limit cell's ability to properly spread and grow. Regarding the effect of incubation of the cell-loaded hydrogels in basal

or osteogenic medium, no significant differences can be seen between the two compositions, which once more shows the composite's ability to sustain the culture of mesenchymal stem cells for long periods of time.

Rheological tests were performed onto hMSCs-embedded hydrogels after incubation for 1 and 14 days under both basal and osteogenic conditions (**Figure 23**). The influence of RGD presence or absence was also investigated (D formulation).

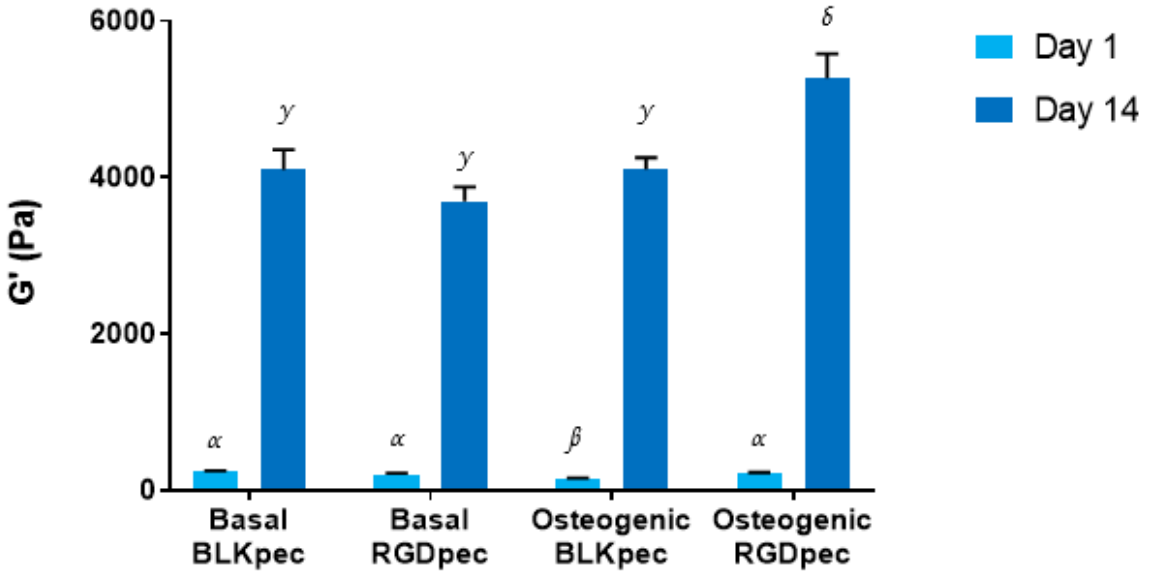

Figure 23 *– Shear modulus - elastic component (G') - values of cell-laden composite hydrogels after incubation for 1 and 14 days under basal and osteogenic conditions. Different symbols denote statistically significant differences between G' values of different formulations for each time-point ($p<0.05$, $n = 4$).*

From the analysis of data shown in **Figure 23**, a very significant increase in G' values after 14 days in culture was clearly noticeable, regardless of the medium in which the samples were incubated in or the type of pectin used. Comparing the results for the same formulation without cells at day 1 (section **4.3.1**), it is possible to infer that the presence of the mesenchymal stem cells translated into a significant decrease in the mechanical properties of the composites. Neves *et al.* (2015) reported similar results to the ones presented here, with hMSCs-laden pectin hydrogels presenting lower shear moduli values comparing to materials without cells, possibly due to the physical interference of cells with the crosslinking process [51]. After 14 days of incubation, even though the formulation using RGDpec under osteogenic presented slightly higher shear modulus

values, every cell-loaded hydrogel exhibited a great increase in G', possibly due to production of matrix. Further assays destined to characterize matrix deposition (such as analysis of collagen and fibronectin) would provide meaningful insight into the cell behaviour inside the composite. It should be noted that no major differences were observed between formulations cultured in the different media, once more showing that the material's own composition provides the necessary ions for gel reinforcement and cell differentiation, removing the need of adding osteogenic supplements.

Finally, to evaluate cell differentiation, namely mineralization induced by the hMSCs, a Von Kossa staining was also performed onto the cell-laden hydrogels. The mineralization was assessed after 7 and 21 days in basal or osteogenic medium (both BLKpec and RGDpec), as displayed in **Figure 24**.

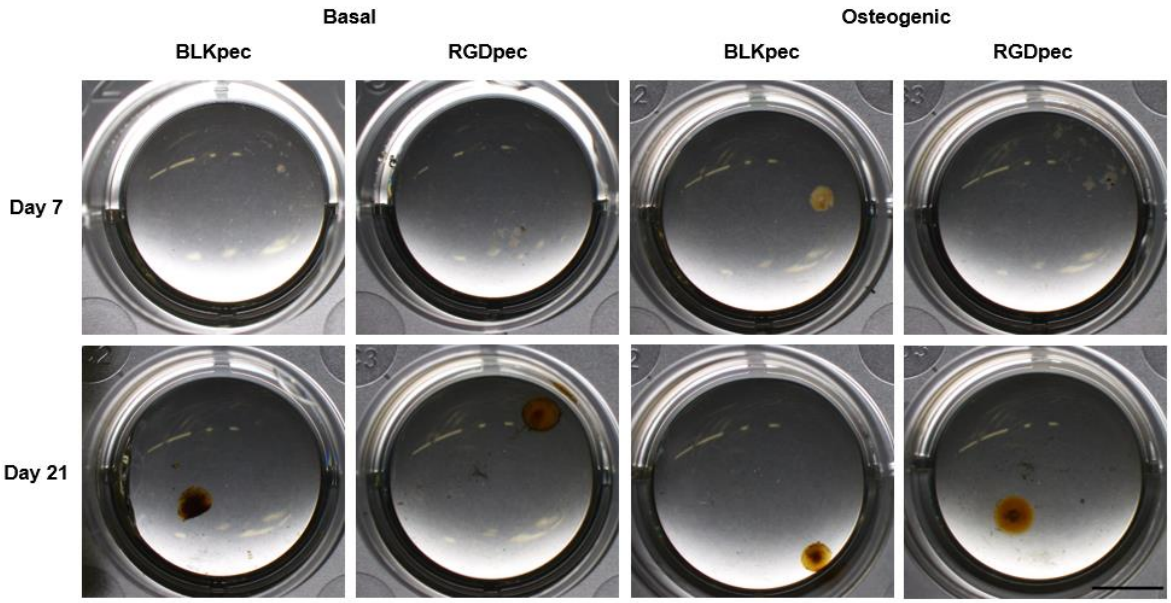

Figure 24 *– Von Kossa staining of hMSC-laden composites after 7 and 21 days of incubation in basal and osteogenic medium (scale bar: 500 μm).*

After analysis of **Figure 24** it can be clearly observed that the staining at day 21 was significantly more intense than at day 7, independently of the culture medium, indicating some level of mineralization even for samples in basal medium, possibly due to the intrinsic osteogenic properties of the bioactive glass, as previously stated. In fact, Kapoor *et al.* (2015) reported similar studies of the differentiation capabilities of the Di-70 with identical results, evidencing positive osteogenic markers for samples incubated with

hMSCs for 21 days without supplements [49]. These results are also consistent with the other tests performed to evaluate the biological behaviour of the embedded hMSCs and the *in vitro* differentiation capabilities of these composite materials, namely the assessment of cell metabolic activity and morphology and the material's rheological properties, which suggested that no osteogenic supplement was needed to induce hMSCs osteogenic differentiation by virtue of the effect of the bioactive glass. In fact, this constitutes an advantage when comparing to pectin hydrogels without bioactive reinforcements, as it has been showed that adequate osteogenic conditions are necessary for the induction of cell differentiation along the osteoblastic lineage and for the nucleation of mineral phases in these cases [60, 62].

Overall, the produced hydrogel-bioactive glass composites proved to display excellent properties for bone tissue engineering, which simultaneously mitigate the drawbacks of both pectin and Di-70 bioactive glass alone. Indeed, the composite hydrogels exhibited the plasticity and versatility of the polymeric phase in addition to the intrinsic osteogenic properties of the ceramic phase, while ensuring a suitable environment for cell entrapment, growth, proliferation and differentiation over several weeks. It was possible to produce materials with tuneable properties and with *in situ* crosslinking ability within clinically relevant timeframes and without resorting to external crosslinking agents. In fact, not only does the material's own composition provide the necessary ions for pectin gelation, but also promotes the differentiation of mesenchymal stem cells without additional osteogenic stimulation, resulting in a biocomposite suitable for bone tissue engineering applications as a cellularized biomaterial.

Chapter 5

Conclusions and Future Work

The present project aimed at fabricating hydrogel-bioactive glass composites, namely based on a pectin matrix, reinforced with bioactive glass particles, aiming at application in bone tissue engineering. The present work allowed to explore the mechanical and biological properties of a novel composite biomaterial, showing some of its advantages and limitations through a process of optimization of manufacturing parameters.

A composite material based on RGD-functionalized pectin and a novel alkali-free formulation of bioactive glass microparticles (formulation of 70% diopside and 30% tricalcium phosphate; Di-70), composed of SiO_2, CaO, MgO and P_2O_5, was successfully prepared, with a set of combined properties constituting an improvement of the original isolated materials: the composite has typically viscoelastic properties of polymers, although is stiffer than pectin alone; in terms of biological behaviour the composite provides an adequate environment for anchorage-dependent cell entrapment provided by RGD-pectin and offers conditions for osteogenic stimulation of stem cells provided by the bioactive glass microparticles.

In fact, the production of materials with tuneable properties was achieved by altering the process parameters (including changes to polymer and glass content and bioactive glass particle size), which allowed for a better understanding of the hydrogel's gelation process and how this affects the final properties of the material, namely their shear modulus values, swelling profile, biological compatibility and differentiation inducing properties. An important result was the production of pectin-based materials without the use of any crosslinking strategy, since crosslinking was provided by the divalent cations released by the bioactive glass used (namely calcium). Cell culture studies demonstrated that these materials are suitable for the entrapment of both fibroblasts and mesenchymal

stem cells (MSC), and promoted their attachment, proliferation and differentiation of MSCs during several weeks. An additional relevant result was the inherent osteogenic character of the materials developed, highly interesting for orthopaedic applications. Cell behaviour in general and differentiation in particular of entrapped MSCs was favoured in basal medium conditions, thus not requiring osteogenic stimulation, probably due to the release of calcium, phosphate and silicon ions from the glass, known for their osteogenicity. Additionally, the improved differentiation further contributed to the mechanical reinforcement of the materials by promoting increased matrix deposition and mineralization.

This work demonstrated that the produced composites might be suitable for an additive manufacturing processing technique, as their controlled self-gelling ability allows for tight regulation of the processing parameters. An additive manufacturing technique such as 3D bioprinting would be of great interest as it allows for an accurate control of cell density in the materials. It would also allow for the production of materials with less batch-to-batch variability, being an automated process, while also promoting scalability.

Additional work should be done in order to better comprehend the composite's interactions with cells and culture medium for longer periods of time, and to mitigate the technical issues encountered throughout the development of this project. In particular, assays destined to characterize matrix deposition (e.g., collagen, fibronectin) by entrapped stem cells are necessary. It would also be interesting to take a step forward and, after the reproduction of several of these tests, try to advance to *in vivo* studies.

Technical and time related restraints limited some of this work's results. For example, ideally, MSCs should have been used in a lower passage to ensure their full differentiation potential, however this was not possible due to the great number of cells needed for the proposed assays.

It would also be interesting to further analyse the composite's structural features, in terms of the polymeric mesh size and the spatial distribution of the bioactive glass particles inside the matrix, by means of scanning electron microscopy and confocal raman microscopy techniques.

Overall, this project's main objective was reached, as the production of a composite biomaterial with potential uses in bone tissue engineering applications was achieved.

Additionally, the produced biocomposite showed promise as a cell-delivery system with *in situ* gelling capabilities within clinically acceptable time frames.

– This page was intentionally left blank –

References

[1] Fiedler, T. *et al.* (2015) "On the mechanical properties of PLC-bioactive glass scaffolds fabricated via BioExtrusion". *Materials Science and Engineering C*, 57: 288-293;

[2] Laurencin, C. T. *et al.* (1999) "Tissue Engineering: Orthopedic Applications". *Annu. Rev. Biomed. Eng.*, 01: 19-46;

[3] Sharifi, E. *et al.* (2016) "Preparation of a biomimetic composite scaffold from gelatin/collagen and bioactive glass fibers for bone tissue engineering". *Materials Science and Engineering C*, 59: 533-541;

[4] Hutmacher, D. W. (2000) "Scaffolds in tissue engineering bone and cartilage". *Biomaterials*, 21: 2529-2543;

[5] O'Brien, F. J. (2011) "Biomaterials & scaffolds for tissue engineering". *Materials Today*, vol. 14, 3: 88-95;

[6] Moreira, H. R. *et al.* (2014) "Injectable pectin hydrogels produced by internal gelation: pH dependence of gelling and rheological properties". *Carbohydrate Polymers*, 103: 339-347;

[7] Pighinelli, L.; Kucharska, M. (2013) "Chitosan-hydroxyapatite composites". *Carbohydrate Polymers*, 93: 256-262;

[8] Salgado, A. J.; Coutinho, O. P.; Reis, R. L. (2004) "Bone Tissue Engineering: State of the Art and Future Trends". *Macromolecular Bioscience*, 4: 743-765;

[9] Tate, P. (2012) "Seeley's Principles of Anatomy and Physiology", 2ª ed. Nova Iorque: McGraw-Hill;

[10] Completo, A.; Fonseca, F. (2011) "Fundamentos de Biomecânica Músculo-esquelética e Ortopédica", Porto: Publindústria;

[11] Gerhardt, L.; Boccaccini, A. R. (2010) "Bioactive Glass and Glass-Ceramic Scaffolds for Bone Tissue Engineering". *Materials*, 3: 3867-3910;

[12] Barrère, F.; Blitterswijk, C. A.; Groot, K. (2006) "Bone Regeneration: molecular and celular interactions with calcium phosphate ceramics". *International Journal of Nanomedicine*, 1(3): 317-332;

[13] Oryan, A. *et al.* (2014) "Bone regenerative medicine: classic options, novel strategies, and future directions". *Journal of Orthopaedic Surgery and Research*, 9:18;

[14] Athanasiou, V. T. *et al*. (2010) "Histological comparison of autograft, allograft-DBM, xenograft, and synthetic grafts in a trabecular bone defect: An experimental study in rabbits". *Med Sci Monit*, 16(1): BR24-31;

[15] Garg, B. *et al*. (2013) "Local distal radius bone graft versus iliac crest bone graft for scaphoid nonunion: a comparative study". *Musculoskelet Surg*, 97: 109-114;

[16] Lee, M.; Song, H.; Yang, K. (2012) "Clinical outcomes of autogenous cancellous bone grafts obtained through the portal for tibial nailing". *Injury, Int. J. Care Injured*, 43: 1118-1123;

[17] Zimmermann, G.; Moghaddam, A. (2011) "Allograft bone matrix versus synthetic bone graft substitutes". *Injury, Int. J. Care Injured*, 42: S16-S21;

[18] Müller, M. A. *et al*. (2013) "Substitutes of structural and non-structural autologous bone grafts in hindfoot arthrodeses and osteotomies: a systematic review". *BMC Musculoskeletal Disorders*, 14: 59-68;

[19] Develioglu, H.; Unver Saraydn, S.; Katal, U. (2009) "The bone-healing effect of a xenograft in a rat calvarial defect model". *Dental Materials Journal*, 28(4): 396-400;

[20] Moshiri, A.; Oryan, A. (2012) "Role of tissue engineering in tendon reconstructive surgery and regenerative medicine: current concepts, approaches and concerns". *Hard Tissue*, 1(2): 11;

[21] Tajbakhsh, S.; Hajiali, F. (2017) "A comprehensive study on the fabrication and properties of biocomposites of poly(lactic acid)/ceramics for bone tissue engineering". Materials Science and Engineering C, 70: 897-912;

[22] Graulus, G.-J. *et al.* (2015) "Cross-linkable alginate-graft-gelatin copolymers for tissue engineering applications". *European Polymer Journal*, 72: 494-506;

[23] Mottaghitalab, F. *et al.* (2015) "Silk as a potencial candidate for bone tissue engineering". *Journal of Controlled Release*, 215:112-128;

[24] Bidarra, S. J. *et al.* (2011) "Injectable *in situ* crosslinkable RGD-modified alginate matrix for endotelial cells delivery". *Biomaterials*, 32: 7897-7904;

[25] Babensee, J. E. *et al*. (1998) "Host response to tissue engineered devices". *Advanced Drug Delivery Reviews*, 33: 111-139;

[26] Yamada, K . M.; Cukierman, E. (2007) "Modeling Tissue Morphogenesis and Cancer in 3D". *Cell*, 130: 601-610;

[27] Jana, S.; Lerman, A. (2015) "Bioprinting a cardiac valve". *Biotechnology Advances*, 33: 1503-1521;

[28] Gomes, M. F. *et al.* (2016) "Homogenous demineralized dentin matrix and platelet-rich plasma for bone tissue engineering in cranioplasty of diabetic rabbits: biochemical, radiographic, and histological analysis". *International Journal of Oral and Maxillofacial Surgery*, 45: 255-266;

[29] Bhattacharjee, P. *et al.* (2016) "Investigating the potential of combined growth factors delivery, from non-mulberry silk fibroin grafted poly(ε-caprolactone)/hydroxyapatite nanofibrous scaffold, in bone tissue engineering". *Applied Materials Today*, 5: 52-67;

[30] Gentile, P. *et al.* (2016) "Localised controlled release of simvastatin from porous chitosan-gelatin scaffolds engrafted with simvastatin loaded PLGA-microparticles for bone tissue engineering application". *Materials Science and Engineering C*, 59: 249-257;

[31] Evangelista, M. B. *et al.* (2007) "Upregulation of bone cell differentiation through immobilization within a synthetic extracelular matrix". *Biomaterials*, 28: 3644-3655;

[32] Maia, F. R. *et al.* (2013) "Functionalization of biomaterials with small osteoinductive moieties". *Acta Biomaterialia*, 9: 8773-8789;

[33] Cao, B.; Liu, N.; Wang, W. (2016) "High glucose prevents osteogenic differentiation of mesenchymal stem cells via lncRNA AK028326/CXCL13 pathway". *Biomedicine & Pharmacotherapy*, 84: 544-551;

[34] Zavaglia, C.A.C.; Silva, M. H. P. (2016) "Feature Article: Biomaterials". Reference Module in *Materials Science and Materials Engineering*;

[35] Inzana, J. A. *et al.* (2016) "Biomaterials approaches to treating implant-associated osteomyelitis". *Biomaterials*, 81: 58-71;

[36] Kurien, T.; Pearson, R. G.; Scammel, B. E. (2013) "Bone graft substitutes currently available in orthopaedic practice". *Bone Joint J.*, 95-B: 583-597;

[37] Inzana, J. A. *et al.* (2015) "3D printed bioceramics for dual antibiotic delivery to treat implant-associated bone infection". *European Cells and Materials*, 30: 232-247;

[38] Koort, J. K. *et al.* (2005) "Efficacy of Ciprofloxacin-Releasing Bioabsorbable Osteoconductive Bone Defect Filler for Treatment of Experimental Osteomyelitis Due to *Staphylococcus aureus*". *Antimicrobial Agents and Chemotherapy*, 49(4): 1502-1508;

[39] Giavaresi, G. *et al.* (2012) "New PMMA-based composites for preparing spacer devices in prosthetic infections". *J Mater Sci: Mater Med*, 23: 1247-1257;

[40] Best, S. M. *et al.* (2008) "Bioceramics: Past, present and for the future". *Journal of the European Ceramic Society*, 28: 1319-1327;

[41] Hutmacher, D. W. *et al.* (2007) "State of the art and future directions of scaffold-based bone engineering from a biomaterials perspective". *J Tissue Eng Regen Med*, 1: 245-260;

[42] Khor, E.; Lim, L. Y. (2003) "Implantable application of chitin and chitosan". *Biomaterials*, 24: 2339-2349;

[43] Cao, W.; Hench, L. L. (1996) "Bioactive Materials". *Ceramics International*, 22: 493-507;

[44] Adams, C. S. *et al.* (2001) "Matrix Regulation of Skeletal Cell Apoptosis". *The Journal of Biological Chemistry*, 278(23): 20316-20322;

[45] Hench, L. L. (2006) "The story of Bioglass®". *J Mater Sci: Mater Med*, 17: 967-978;

[46] Goel, A. *et al.* (2012) "Alkali-free bioactive glasses for bone tissue engineering: A preliminary investigation". *Acta Biomaterialia*, 8:361-372;

[47] Hench, L. L. (1991) "Bioceramics: From Concept to Clinic". *J. Am. Ceram. Soc.*, 74(7): 1487-1510;

[48] Junior, P. E. S.; Oréfice, R. L. (2001) "Compósitos Bioativos Obtidos a Partir da Inserção de Vidro Bioativo em matriz de Poli(Metacrilato de Metila)". *Polímeros: Ciência e Tecnologia*, 11(3): 109-115;

[49] Kapoor, S. *et al.* (2015) "Understanding the composition-structure-bioactivity relationships in diopside ($CaO{\cdot}MgO{\cdot}2SiO_2$)–tricalcium phosphate ($3CaO{\cdot}P_2O_5$) glass system". *Acta Biomaterialia*, 15: 210-226;

[50] Kapoor, S. *et al.* (2015) "Alkali-free bioactive diopside-tricalcium phosphate glass-ceramics for scaffold fabrication: Sintering and crystallization behaviours". *Journal of Non-Crystalline Solids*, 432: 81-89;

[51] Neves, S. C. *et al.* (2015) "Biofunctionalized pectin hydrogels as 3D celular microenvironments". *Journal of Materials Chemistry B*, 3: 2096-2108;

[52] Villanova, J. C. O.; Ayres, E.; Oréfice, R. L. (2015) "Design, characterization and preliminar *in vitro* evaluation of a mucoadhesive polymer based on modified pectin and acrylic monomers with potential use as a pharmaceutical excipient". *Carbohydrate Polymers*, 121: 372-381;

[53] Munarin, F.; Tanzi, M. C.; Petrini, P. (2012) "Advances in biomedical applications of pectin gels". *International Journal of Biological Macromolecules*, 51:681-689;

[54] Kumar, P. T. *et al.* (2013) "Drug delivery and tissue engineering applications of biocompatible pectin-chitin/nano $CaCO_3$ composite scaffolds". *Colloids and Surfaces B: Biointerfaces*, 106: 109-116;

[55] Ventura, I.; Jammal, J.; Bianco-Peled, H. (2013) "Insights into the nanostructure of low-methoxyl pectin-calcium gels". *Carbohydrate Polymers*, 97: 650-658;

[56] Coimbra, P. *et al.* (2011) "Preparation and chemical and biological characterization of a pectine/chitosan polyelectrolyte complex scaffold for possible bone tissue engineering applications". *International Journal of Biological Macromolecules*, 48: 112-118;

[57] Sivashanmugam., A. *et al.* (2015) "An overview of injectable polymeric hydrogels for tissue engineering". *European Polymer Journal*, 72: 543-565;

[58] Braccini, I.; Pérez, S. (2011) "Molecular Basis of Ca^{2+}-Induced Gelation in Alginates and Pectins: The Egg-Box Model Revisited". *Biomacromolecules*, 2: 1089-1096;

[59] Rowley, J. A.; Madlambayan, G.; Mooney, D. J. (1999) "Alginate hydrogels as synthetic extracellular matrix materials". *Biomaterials*, 20: 45-53;

[60] Munarin, F. *et al.* (2010) "Mineral phase deposition on pectin microspheres". *Materials Science and Engineering C*, 30: 491-496;

[61] Maia, F. R. *et al.* (2014) "Hydrogel depots for local co-delivery of osteoinductive peptides and mesenchymal stem cells". *Journal of Controlled Release*, 189: 158-168;

[62] Munarin, F. *et al.* (2011) "Pectin-based Injectable Biomaterials for Bone Tissue Engineering". *Biomacromolecules*, 12: 568-577;

[63] Maia, F. R. *et al.* (2014) "Matrix-driven formation of mesenchymal stem cell-extracellular matrix microtissues on soft alginate hydrogels". *Acta Biomaterialia*, 10: 3197-3208;

[64] Munarin, F. *et al.* (2014) "Reactive hydroxyapatite fillers for pectin biocomposites" *Materials Science and Engineering C*, 45: 154-161;

[65] Gantar, A. *et al.* (2014) "Nanoparticulate bioactive-glass-reinforced gellan-gum hydrogels for bone-tissue engineering". *Materials Science and Engineering C*, 43: 27-36;

[66] Jia, W. *et al.* (2010) "Novel borate glass/chitosan composite as a delivery vehicle for teicoplanin in the treatment of chronic osteomyelitis". *Acta Biomaterialia*, 6: 812-819;

[67] Chen, Q.; Roether, J. A.; Boccaccini, A. R. (2008) "Tissue Engineering Scaffolds from Bioactive Glass and Composite Materials" In N. Ashammakhi, R. Reis & F. Chiellini (Eds.) *Topics in Tissue Engineering*, Vol. 4;

[68] Ribeiro, M. *et al.* (2015) "Development of silk fibroin/nanohydroxyapatite composite hydrogels for bone tissue engineering". *European Polymer Journal*, 67: 66-77;

[69] Kong, L. *et al.* (2006) "A study on the bioactivity of chitosan/nano-hydroxyapatite composite scaffolds for bone tissue engineering". *European Polymer Journal*, 42: 3171-3179;

[70] Killion, J. A. *et al.* (2013) "Hydrogel/bioactive glass composites for bone regeneration applications: Synthesis and characterisation". *Materials Science and Engineering C*, 33: 4203-4212;

[71] Sohrabi, M. *et al.* (2013) "Development of injectable biocomposites from hyaluronic acid and bioactive glass nano-particles obtained from diferente sol-gel routes". *Materials Science and Engineering C*, 33: 3730-3744;

[72] Munarin, F. *et al.* (2015) "Micro- and nano-hydroxyapatite as active reinforcement for soft biocomposites". *International Journal of Biological Macromolecules*, 72: 199-209;

[73] Misra, S. K. *et al.* (2008) "Comparison of nanoscale and microscale bioactive glass on the properties of P(3HB)/Bioglass® composites". *Biomaterials*, 29: 1750-1761;

[74] Maji, K. *et al.* (2015) "Preparation and Evaluation of Gelatin-Chitosan-Nanobioglass 3D Porous Scaffold for Bone Tissue Engineering". *International Journal of Biomaterials*, Volume 2016: 14 pages;

[75] Marelli, B. *et al.* (2010) "Three-Dimensional Mineralization of Dense Nanofibrillar Collagen-Bioglass Hybrid Scaffolds". *Biomacromolecules*, 11: 1470-1479;

[76] Mota, J. *et al.* (2012) "Chitosan/bioactive glass nanoparticle composite membranes for periodontal regeneration". *Acta Biomaterialia*, 8: 4173-4180;

[77] Merelli, B. *et al.* (2011) "Accelerated mineralization of dense collagen-nano bioactive glass hybrid gels increases scaffold stiffness and regulates osteoblastic function". *Biomaterials*, 32, 8915-8926;

[78] Leite, A. J. *et al.* (2016) "Bioplotting of a bioactive alginate dialdehyde-gelatin composite hydrogel containing bioactive glass nanoparticles". *Biofabrication*, 8: 035005;

[79] Gao, W. *et al.* (2015) "The status, challenges, and future of additive manufacturing in engineering". *Computer-Aided Design*, 69: 65-89;

[80] Miranda, P. *et al.* (2006) "Sintering and robocasting of β-tricalcium phosphate scaffolds for orthopaedic applications". *Acta Biomaterialia*, 2: 457-466;

[81] Klein, J. *et al.* (2015) "Additive Manufacturing of Optically Transparent Glass". *3D Printing and Additive Manufacturing*, Volume 2, 3: 92-105;

[82] Munarin, F. *et al.* (2012) "Biofunctional chemically modified pectin for cell delivery". *Soft Matter*, 8: 4731-4739;

[83] Fu, D. *et al.* (2008) "Preparation and property analysis of polyacrylate dispersant for calcium carbonate". *Colloids and Surfaces A: Physicochemical and Engineering Aspects*, 326: 122-128;

[84] Cafarelli, A. *et al.* (2016) "Tuning acoustic and mechanical properties of materials for ultrasound phantoms and smart substrates for cell cultures". *Acta Biomaterialia*, Accepted Manuscript;

[85] Vetsch, J. R. *et al.* (2015) "Effect of fetal bovine serum on mineralization on silk fibroin scaffolds". *Acta Biomaterialia*, 13: 277-285;

[86] Zhou, M. *et al.* (2009) "Self-assembled peptide-based hydrogels as scaffolds for anchorage-dependent cells". *Biomaterials*, 30: 2523-2530;

[87] Zhai, W. *et al.* (2013) "Stimulatory effects of the ionic products from Ca-Mg-Si bioceramics on both osteogenesis and angiogenesis in vitro". *Acta Biomaterialia*, 9: 8004-8014.

Annexes

I – Calibration curve for RGD-grafting quantification

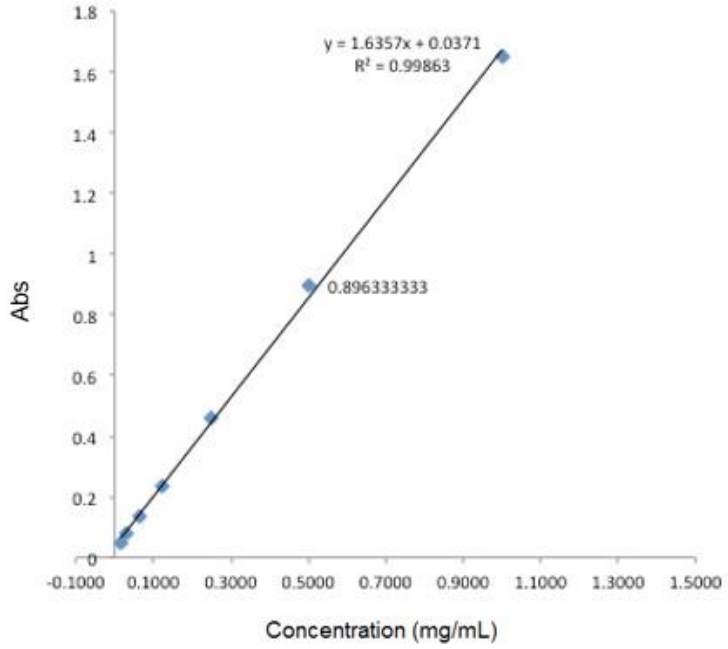

Figure A1 *– Calibration curve of absorbance values of pectin solutions containing increasingly higher RGD concentrations*

Annexes

II – Calibration curves for the quantification of Di-70's components in complete α-MEM

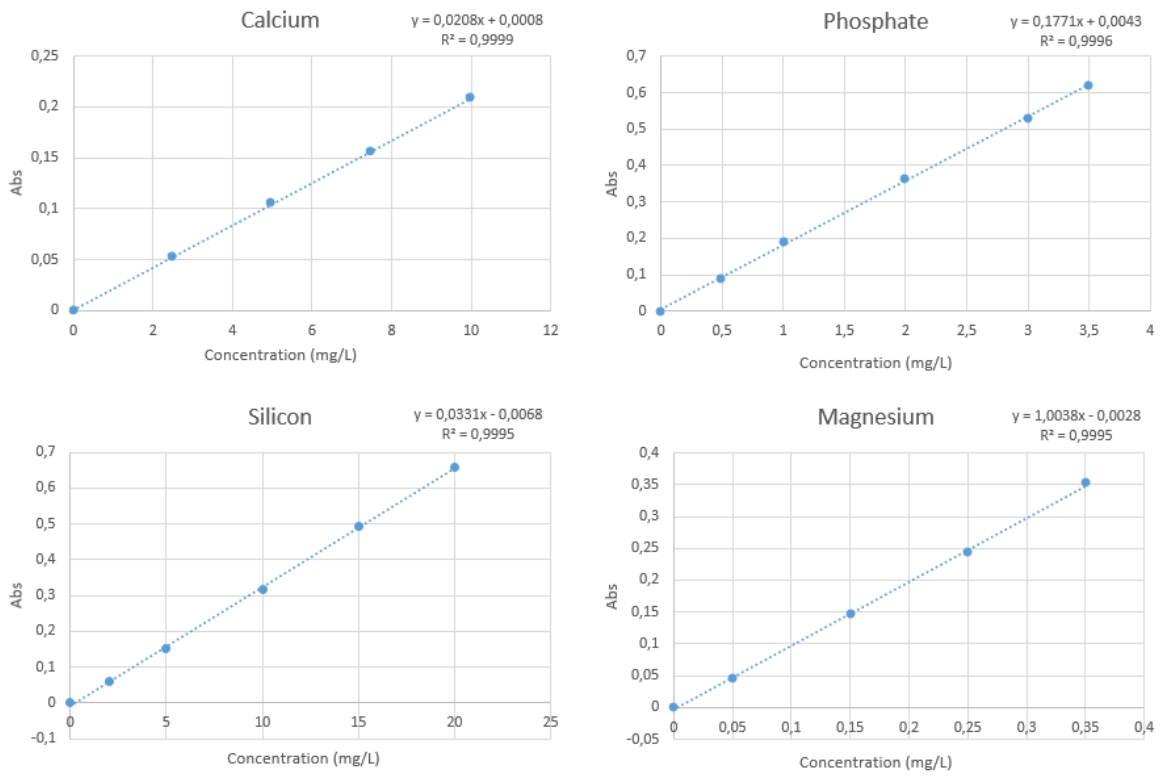

Figure A2 – *Calibration curves of absorbance vs. different concentrations of calcium, phosphate, silicon and magnesium through spectrophotometric methods.*

Annexes

III – Table of statistical analysis of data from Figure 19

Parameter 1	vs	Parameter 2	Statistical Significance
Day 1 – C – BLKpec	vs	Day 1 – C – RGDpec	n.s.
Day 1 – C – BLKpec	vs	Day 1 – D – BLKpec	*
Day 1 – C – BLKpec	vs	Day 1 – D – RGDpec	*
Day 1 – C – BLKpec	vs	Day 7 – C – BLKpec	*
Day 1 – C – RGDpec	vs	Day 1 – D – BLKpec	n.s.
Day 1 – C – RGDpec	vs	Day 1 – D – RGDpec	n.s.
Day 1 – C – RGDpec	vs	Day 7 – C – RGDpec	*
Day 1 – D – BLKpec	vs	Day 1 – D – RGDpec	n.s.
Day 1 – D – BLKpec	vs	Day 7 – D – BLKpec	*
Day 1 – D – RGDpec	vs	Day 7 – D – RGDpec	*
Day 7 – C – BLKpec	vs	Day 7 – C – RGDpec	*
Day 7 – C – BLKpec	vs	Day 7 – D – BLKpec	*
Day 7 – C – BLKpec	vs	Day 7 – D – RGDpec	*
Day 7 – C – RGDpec	vs	Day 7 – D – BLKpec	*
Day 7 – C – RGDpec	vs	Day 7 – D – RGDpec	*
Day 7 – D – BLKpec	vs	Day 7 – D – RGDpec	n.s.

Legend: * mark denotes statistical differences ($p<0.05$); n.s. means not statistically significant.

Annexes

IV – Table of statistical analysis of data from Figure 21

Parameter 1	vs	Parameter 2	Statistical Significance
Day 1 – Basal – BLKpec	vs	Day 1 – Basal – RGDpec	n.s.
Day 1 – Basal – BLKpec	vs	Day 1 – Osteogenic – BLKpec	n.s.
Day 1 – Basal – BLKpec	vs	Day 1 – Osteogenic – RGDpec	*
Day 1 – Basal – BLKpec	vs	Day 14 – Basal – BLKpec	*
Day 1 – Basal – BLKpec	vs	Day 21 – Basal – BLKpec	*
Day 1 – Basal – RGDpec	vs	Day 1 – Osteogenic – BLKpec	n.s.
Day 1 – Basal – RGDpec	vs	Day 1 – Osteogenic – BLKpec	n.s.
Day 1 – Basal – RGDpec	vs	Day 14 – Basal – RGDpec	n.s.
Day 1 – Basal – RGDpec	vs	Day 21 – Basal – RGDpec	n.s.
Day 1 – Osteogenic – BLKpec	vs	Day 1 – Osteogenic – RGDpec	n.s.
Day 1 – Osteogenic – BLKpec	vs	Day 14 – Osteogenic – BLKpec	*
Day 1 – Osteogenic – BLKpec	vs	Day 21 – Osteogenic – BLKpec	*
Day 1 – Osteogenic – RGDpec	vs	Day 14 – Osteogenic – RGDpec	n.s.
Day 1 – Osteogenic – RGDpec	vs	Day 21 – Osteogenic – RGDpec	n.s.
Day 14 – Basal – BLKpec	vs	Day 14 – Basal – RGDpec	*
Day 14 – Basal – BLKpec	vs	Day 14 – Osteogenic – BLKpec	*
Day 14 – Basal – BLKpec	vs	Day 14 – Osteogenic – RGDpec	*
Day 14 – Basal – BLKpec	vs	Day 21 – Basal – BLKpec	n.s.
Day 14 – Basal – RGDpec	vs	Day 14 – Osteogenic – BLKpec	*

Parameter 1	vs	Parameter 2	Statistical Significance
Day 14 – Basal – RGDpec	vs	Day 14 – Osteogenic – RGDpec	n.s.
Day 14 – Basal – RGDpec	vs	Day 21 – Basal – RGDpec	n.s.
Day 14 – Osteogenic – BLKpec	vs	Day 14 – Osteogenic – RGDpec	*
Day 14 – Osteogenic – BLKpec	vs	Day 21 – Osteogenic – BLKpec	*
Day 14 – Osteogenic – RGDpec	vs	Day 21 – Osteogenic – RGDpec	n.s.
Day 21 – Basal – BLKpec	vs	Day 21 – Basal – RGDpec	n.s.
Day 21 – Basal – BLKpec	vs	Day 21 – Osteogenic – BLKpec	*
Day 21 – Basal – BLKpec	vs	Day 21 – Osteogenic – RGDpec	*
Day 21 – Basal – RGDpec	vs	Day 21 – Osteogenic – BLKpec	*
Day 21 – Basal – RGDpec	vs	Day 21 – Osteogenic – RGDpec	n.s.
Day 21 – Osteogenic – BLKpec	vs	Day 21 – Osteogenic – RGDpec	*

Legend: * mark denotes statistical differences ($p<0.05$); n.s. means not statistically significant.